PUBLISHER :

Address of Publisher & Editor's Office :

GDAŃSK UNIVERSITY
OF TECHNOLOGY
Faculty
of Ocean Engineering
& Ship Technology

ul. Narutowicza 11/12
80-952 Gdańsk, POLAND
tel.: +48 58 347 17 93
fax : +48 58 341 47 12
e-mail : sekoce@pg.gda.pl

Account number :
BANK ZACHODNI WBK S.A.
I Oddział w Gdańsku
41 1090 1098 0000 0000 0901 5569

Editorial Staff :
Witold Kirkor Editor in Chief
e-mail : pmrs@op.pl
Przemysław Wierzchowski Scientific Editor
e-mail : e.wierzchowski@chello.pl
Maciej Pawłowski Editor for review matters
e-mail : mpawlow@pg.gda.pl
Tadeusz Borzęcki Editor for international relations
e-mail : tadbor@pg.gda.pl
Cezary Spigarski Computer Design
e-mail : biuro@oficynamorska.pl

Domestic price :
single issue : 20 zł

Prices for abroad :
single issue :
- in Europe EURO 15
- overseas US$ 20

ISSN 1233-2585

POLISH MARITIME RESEARCH

in internet

www.bg.pg.gda.pl/pmr.html

Index and abstracts of the papers 1994 ÷ 2004

POLISH MARITIME RESEARCH

No 4(46) 2005 Vol 12

CONTENTS

The papers published in this issue have been reviewed by :
Prof. T. Koronowicz ; Prof. J. Lisowski
Prof. K. Rosochowicz ; Assoc.Prof. M. Sperski
Prof. K. Wierzcholski

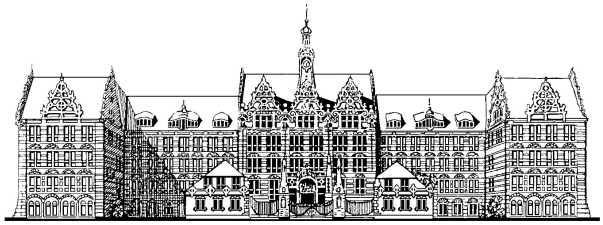

1904 1945 2004/2005

JUBILEE ACADEMIC YEAR 2004/2005
60 YEARS OF GDAŃSK UNIVERSITY OF TECHNOLOGY

Editorial

POLISH MARITIME RESEARCH is a scientific journal of worldwide circulation. The journal appears as a quarterly four times a year. The first issue of it was published in September 1994. Its main aim is to present original, innovative scientific ideas and Research & Development achievements in the field of :

Engineering, **Computing & Technology**, **Mechanical Engineering**,

which could find applications in the broad domain of maritime economy. Hence there are published papers which concern methods of the designing, manufacturing and operating processes of such technical objects and devices as : ships, port equipment, ocean engineering units, underwater vehicles and equipment as well as harbour facilities, with accounting for marine environment protection.
The Editors of POLISH MARITIME RESEARCH make also efforts to present problems dealing with education of engineers and scientific and teaching personnel. As a rule, the basic papers are supplemented by information on conferences , important scientific events as well as cooperation in carrying out international scientific research projects.

Editorial Board

The effect of limited depth and width of waterway on performance of ducted propellers

Wojciech Górski
Ship Design and Research Centre S.A., Gdańsk

Jan Kulczyk, Tomasz Tabaczek
Wrocław University of Technology

ABSTRACT

Model tests of propeller performance in bollard conditions, in deep and shallow water, were carried out at Ship Design and Research Centre in Gdańsk. Corresponding calculations of propeller performance with account for finite dimensions of canal cross-section were carried out at Wrocław University of Technology by using their own theoretical model of propeller – hull interaction. The calculations were carried out in model scale, at the same water depth as in model tests. For given hull form, propeller geometry and canal cross--section the HPSDK computer code was used to calculate wake fraction, as well as propeller thrust, torque and efficiency. The distribution of pressure on waterway bottom and ship sinkage were also determined.

Keywords : inland navigation, performance of ducted propeller

INTRODUCTION

The effect of limited depth and width of waterway on the performance of propellers, as is the case in inland navigation, have not been by now extensively reported in the literature. In the RTD project INBAT the above problem was considered important, for it is related to efficiency of propulsion. In order to investigate mutual interaction of ship and waterway both experimental and theoretical research tools were involved. Because of confinements imposed by actual diameters of stock propellers used in tests and large dimensions of model ship the model tests in shallow water were limited to bollard conditions (zero speed). Theoretical CFD methods do not impose limits on dimensions. However, many simplifications applied to the computational method, both to geometry and governing equations, make the applicability of those methods restricted. In the present investigations the experimental and theoretical methods were applied to the same ship at the same operating conditions, and provided with complementary information. Theoretical calculations were carried out in model scale in order to avoid extrapolation errors when analyzing results.

HPSDK COMPUTER CODE

When developing the HPSDK code it was assumed that hull, propeller (either screw propeller or ducted propeller) and waterway bed (banks and bottom) are considered separately, and their interaction is taken into account by using iterative solution of flow including updated disturbances. That approach was forced by low computational power of available hardware. 3-D potential flow bounded by ship hull, rigid water surface and canal bed is calculated using the technique of surface vorticity distribution. Viscous effect on velocity distribution in propeller disk is taken into account by simplified calculation of viscous flow between hull and canal bottom. The Vortex Lattice Method was applied to propeller flow at a given distribution of inflow velocity. The above mentioned methods are described in details in [1] and [2]. The flow chart of calculations is presented in Fig.1.

The computations are organized in 5 steps :

Step 1

Within this step the necessary input data are prepared for calculations. Hull form is defined and processed in SIATKA module. The data file is next read by the HPSEDKDB data editor that allows to enter a number of complementary data such as : water depth, dimensions of canal cross-section, ship speed, propeller diameter and the number of vortex panels representing water surface around the ship. The HPSEDSRC editor is dedicated to propeller geometry, and the HPSEDDSA editor to nozzle geometry in the case of ducted propeller.On the basis of the entered hull form the VORNET module computes the coordinates of grid representing the hull in subsequent calculations. The TARCIE module calculates the effect of viscosity on distribution of flow velocity under the hull.

Step 2

The HDKDK and HDKRK modules calculate potential flow around the ship and wake fraction, respectively. If the goal of calculations is to determine the nominal flow (excluding the effect of running propeller), the HDKRK module computes pressure distribution on the canal bottom, then ship sinkage is determined and the calculations are terminated. If the goal is to determine the effective flow and performance of propeller the

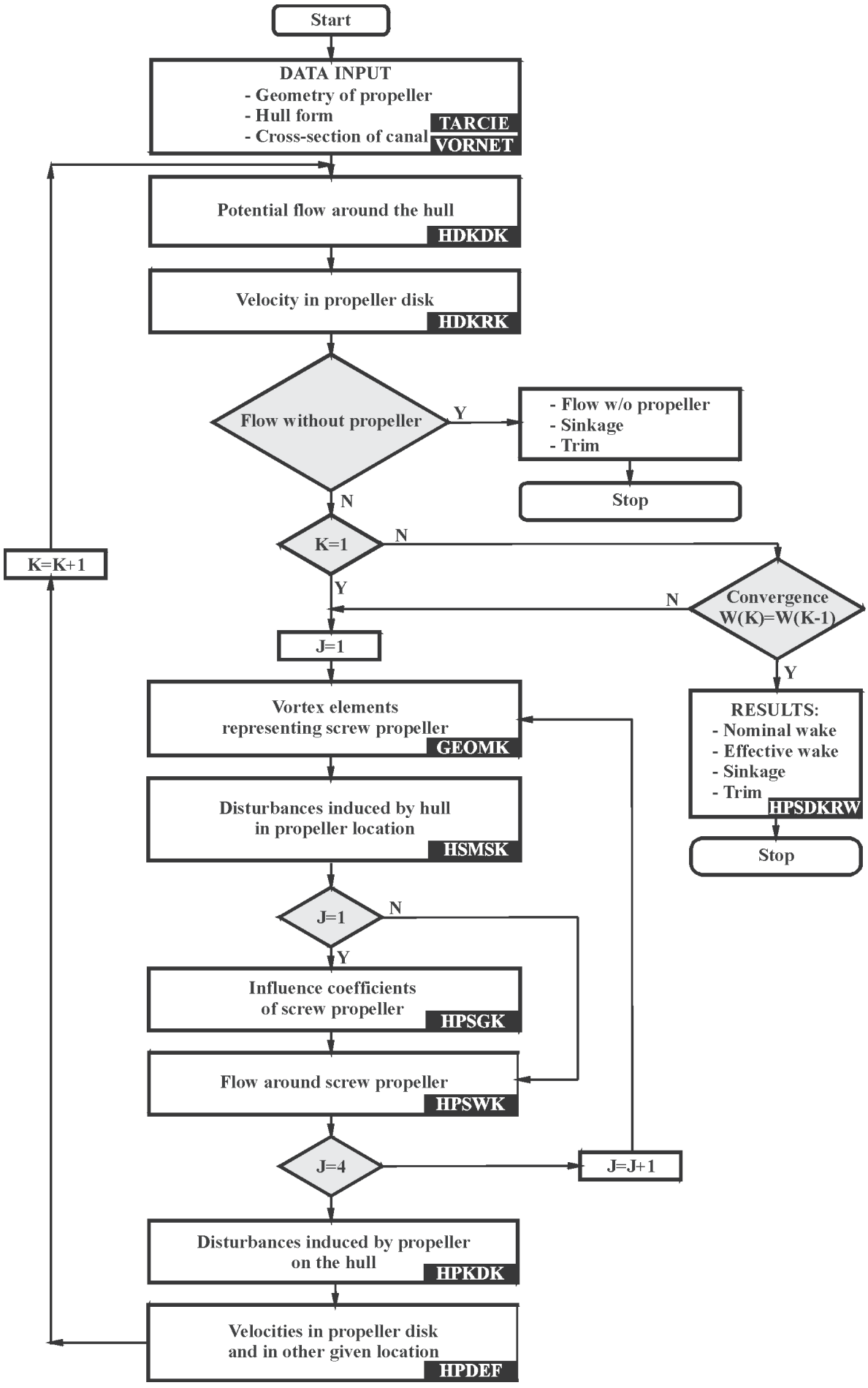

Fig. 1. Flow chart of computations carried out by the HPSDK code

iterative procedure must be completed and the remaining steps are pursued. The calculated flow field including viscous effects is used as input to propeller flow calculation in the next steps.

Step 3

Propeller data are prepared for solving the flow around propeller (the modules : GEOMK, HSMDK, HPDSK, HPSGK, HPDGK). A grid of vortex elements representing propeller blades and nozzle is defined and the coefficients of governing equations are computed. The effects of hull and waterway bottom are taken into account by calculating the velocity induced by vortex elements representing hull and bottom in collocation points on propeller.

Step 4

Flow around screw propeller is solved by the HPSWK module. In the case of a ducted propeller the flow is solved by the HPSWK and HPDWK modules running alternately. The HPSWK module computes the flow around impeller including disturbances (velocities) induced by nozzle. The HPDWK module solves the flow around nozzle including disturbances induced by the impeller. In the case of a hull-integrated nozzle the sector located inside the hull outline is disregarded in computations. No special adjustment is made in the area of the junction. The process of alternate solving the flows around impeller and nozzle is not illustrated in the flow chart shown in Fig.1. Thrust and torque are calculated by integrating the pressure on impeller blades and nozzle.

Step 5

Velocities induced by propeller are computed in collocation points on hull (by HPKDK module) and in propeller disk (by HPDEF module). Effective wake fraction is calculated by HDKRK module.

At this point the convergence of the iterative procedure is tested by using the values of effective wake fraction computed in the present and previous runs of HDKRK module. If the relative difference in wake fraction is less than 0.05 then computations are terminated. The above convergence value is usually reached after 2 or 3 calculation loops including steps 3 through 5. The values of thrust and torque are averaged because the results oscillate.

Propeller performance, distribution of hull pressure, distribution of bottom pressure, ship sinkage and velocity distribution in flow with and without the effect of running propeller are presented below.

PROPELLER PERFORMANCE IN BOLLARD CONDITIONS

Model tests of bollard pull were carried out at Ship Design and Research Centre by using the pushboat model in the scale of 1:4.72. The full-scale dimensions of the pushboat were as follows :

Length overall : L_{OAp} = 20.5 m
Moulded beam : B_p = 9.0 m
Moulded draught : d_p = 0.6 m

The hull form of the pushboat is shown in Fig.2. The pushboat was propelled by three propellers because of the limited draught and variable thrust demand depending on a number of barges, draught of barges and water depth. Two side propellers were the ducted ones with hull-integrated nozzle. The diameter of the model propellers used in tests corresponded to 0.690 m in full scale. The stock propellers were applied of Ka 4 -70 Wageningen propeller series, running in 19A nozzle. The central propeller was designed as a ducted propeller of Z-drive azimuthing arrangement. It is lowered to operating position at a water depth greater than 1.2 m, and retracted when water depth is smaller than that. The diameter of the central propeller was equal to 1.100 m. In the model tests the CP324 stock propeller in nozzle 19A was applied [3].

Corresponding computations were carried out for the train composed of two barges and the pushboat in model scale. Main particulars of a single barge were as follows :

L_{OAb} = 48.75 m
B_b = 9.00 m
d_b = 1.40 m

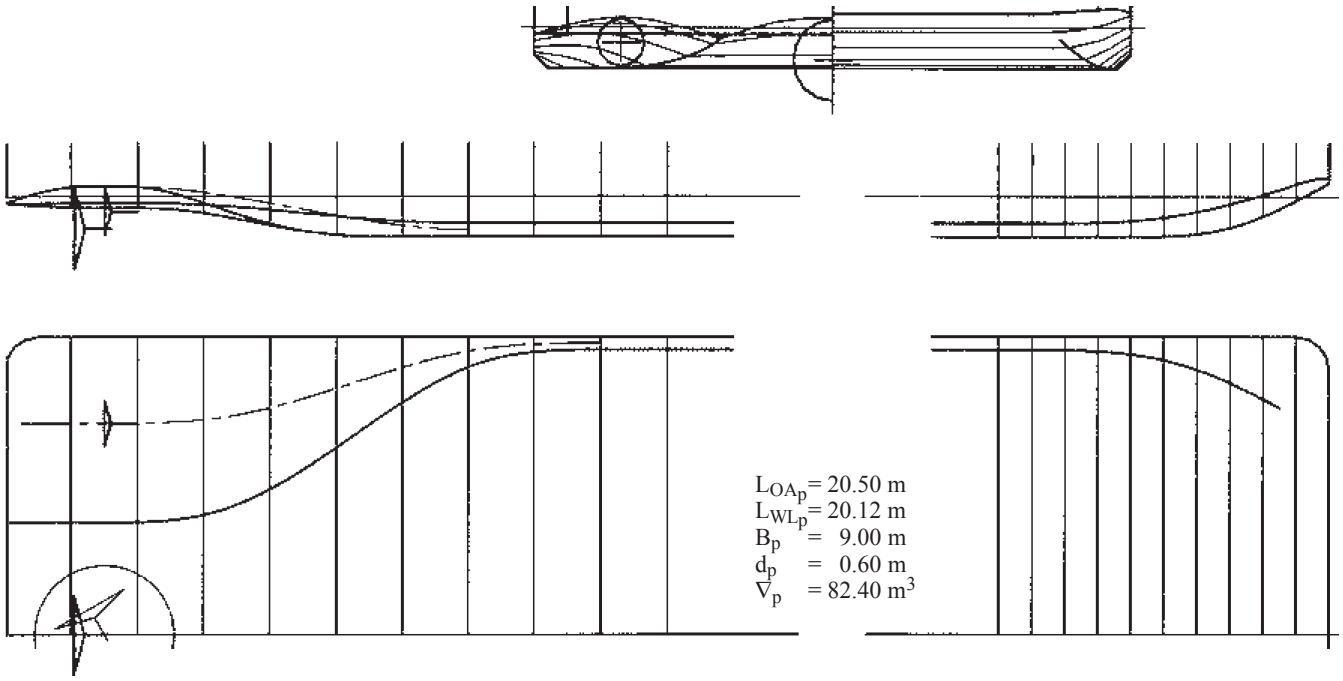

Fig. 2. *Hull form of the pushboat used for model tests and computations*

Propeller performance

Results of the model tests and computations are compared in Tab.1. The HPSDK code is not capable of computing the propeller performance exact in bollard conditions i.e. at zero ship speed. In order to overcome the problem the computations were run at low ship speed values, namely at 0.75 m/s, 0.50 m/s, 0.25 m/s, and a constant rotational speed of propellers. Propeller performance was then extrapolated to zero ship speed. The relationship between ship speed and propeller thrust appeared almost linear for both central and side propellers (Fig. 3). The results are consistent with hydrodynamic characteristics of the propellers.

Tab. 1. *Thrust of the propeller and pull of the pushboat in bollard conditions*

Propeller		Central				Side*			
Water depth		2m		5m		2m		5m	
Rotational speed [rps]		12.5	7.5	12.5	7.5	30	20	30	20
Model tests	Thrust of impeller [N]	-	-	-	-	164.9	72.6	173.5	74.6
	Thrust [N]	240.8	90.4	225.6	90.5	-	-	-	-
	Pull [N]	218.1	73.8	208.8	82.1	273.5	109.9	296.1	132.8
Computations	Thrust of impeller [N]	-	-	-	-	178	80	178	80
	Thrust [N]	211	76	208	74	256	115	260	116

* Total thrust of the two impellers is given in the table

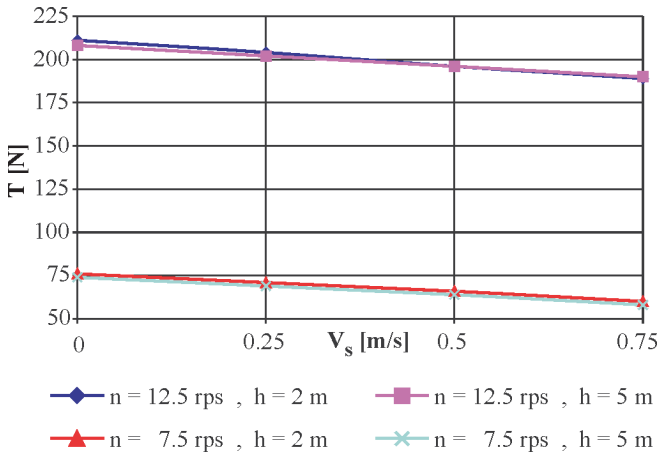

Fig. 3. *Thrust of the central propeller, extrapolated to bollard conditions*

The following magnitudes were measured during the model tests :

- the net thrust of the entire central propulsion unit (including shaft post in front of the propeller)
- the thrust of the side impellers (excluding the thrust of nozzle), and
- the pull of the pushboat [4].

In the computational model the shaft post in front of the propeller was not accounted for. The computed thrust of the central propeller, shown in Tab.1, contains only the thrust generated by impeller and nozzle.

Both the results of the model tests and computations revealed that the effect of water depth on thrust and pull at zero ship speed is insignificant.

Bottom pressure

The computations revealed that at the water depth of 2.0 m the central propeller induces, at the beginning of stern tunnels (x = -1.1m), a higher drop of pressure than side propellers (Fig.4). The results seem reasonable because the central propeller is closer to the waterway bottom than the side propellers. For smaller depths one may expect even a higher drop of bottom pressure and thus a greater destructive effect of running propeller on waterway bottom. This regularity is illustrated in Fig.5 for the side propellers. The results of computations also showed that the rotational speed of propellers within the considered range had no effect on the distribution of bottom pressure.

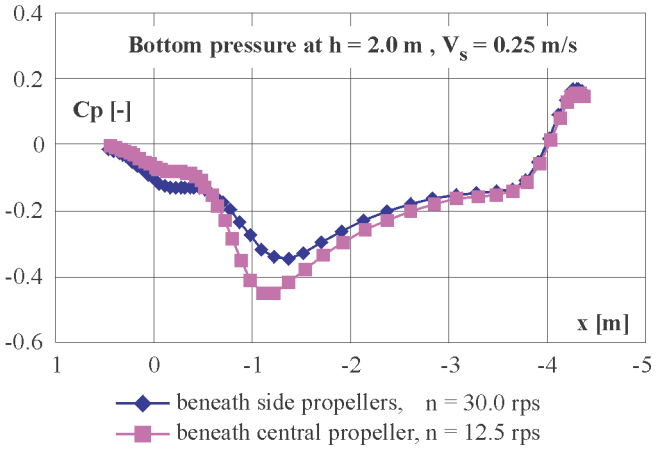

Fig. 4. *Distribution of bottom pressure at near zero ship speed (stern transom at x = 0; side propellers at x = - 0.318; central propeller at x = - 0.234)*

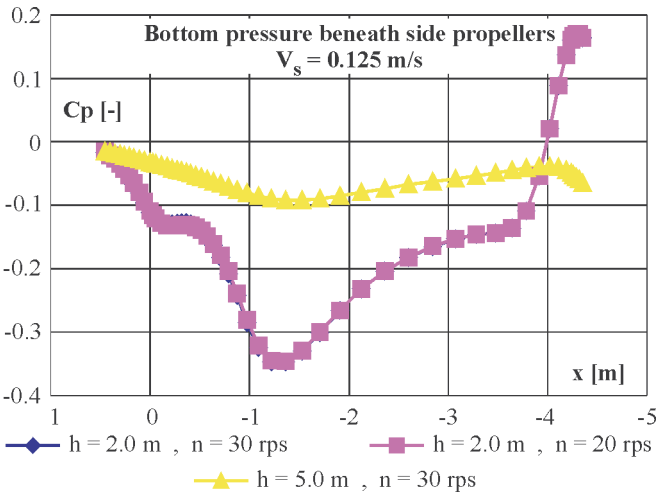

Fig. 5. *The effect of water depth and propeller's rotational speed on the distribution of bottom pressure beneath side propeller at near zero ship speed (stern transom at x = 0; side propellers at x = - 0.318)*

THE EFFECT OF CANAL CROSS-SECTION ON PROPELLER PERFORMANCE

The computations of propeller performance in the canal of trapezoidal cross-section were carried out in the scale of 1:14. The slope of banks was 1: 4. The draught of barges was assumed equal to 1.4 m. In the computations the barge train was positioned in various distances from the banks (Fig. 6). For the considered pushboat the computations were carried out separately for the central and side propellers as the interaction between propellers was experimentally proven negligible.

The results for ship scale are presented in Tab.2 and 3. The canal width b_0 is measured at the canal bottom. The advance coefficient J was calculated with account for the effective wake fraction w_e.

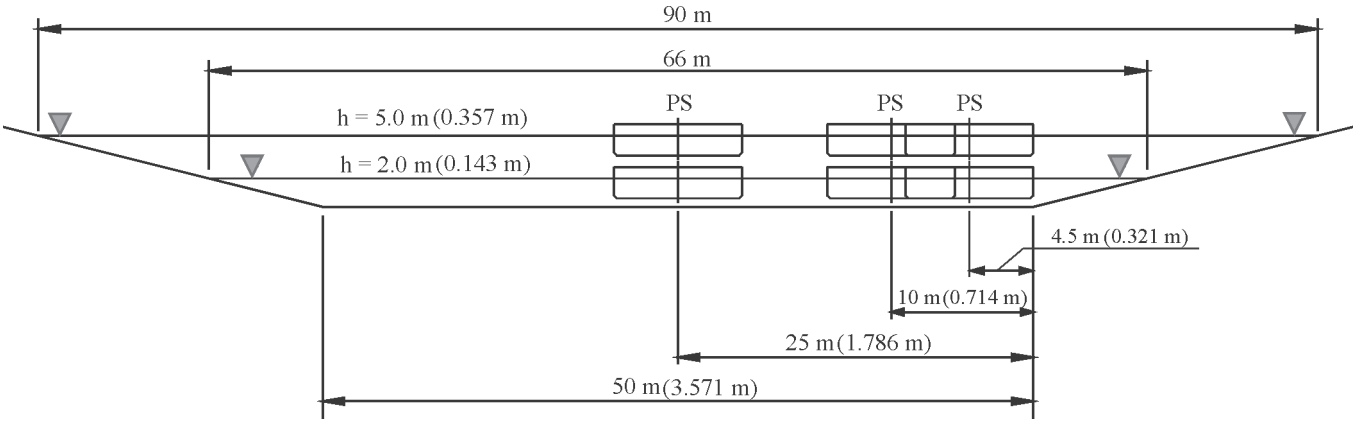

Fig.6. *Cross-section of the canal and considered positions of the barge train*

Tab. 2. *Performance of the side propeller in the canal (the propeller's diameter D = 0.690 m, and its rotational speed n = 828.5 rpm)*

Water depth h = 1.7 m						
Canal width b_0	9 m		20 m		50 m	
Ship speed V_S [m/s]	1.5	3.0	1.5	3.0	1.5	3.0
Nominal wake fraction w_n	0.289	0.523	0.243	0.475	0.109	0.331
Effective wake fraction w_e	0.834	0.753	0.788	0.707	0.640	0.558
Thrust coeff. K_T	0.331	0.319	0.330	0.315	0.325	0.303
Efficiency η	0.050	0.127	0.062	0.147	0.092	0.212
Advance coeff. J	0.030	0.080	0.038	0.094	0.057	0.142
Water depth h = 2.0 m						
Canal width b_0	9 m		20 m		50 m	
Ship speed V_S [m/s]	1.5	3.0	1.5	3.0	1.5	3.0
Nominal wake fraction w_n	0.632	0.588	0.672	0.629	0.778	0.74
Effective wake fraction w_e	0.190	0.411	0.220	0.449	0.345	0.577
Thrust coeff. K_T	0.296	0.274	0.305	0.293	0.311	0.304
Efficiency η	0.198	0.283	0.184	0.254	0.158	0.203
Advance coeff. J	0.127	0.188	0.122	0.175	0.103	0.135
Water depth h = 3.6 m						
Canal width b_0	9 m		20 m		50 m	
Ship speed V_S [m/s]	1.5	3.0	1.5	3.0	1.5	3.0
Nominal wake fraction w_n	0.222	0.216	0.250	0.244	0.302	0.296
Effective wake fraction w_e	- 0.285	- 0.004	- 0.279	0.009	- 0.23	0.060
Thrust coeff. K_T	0.265	0.217	0.282	0.255	0.284	0.259
Efficiency η	0.293	0.417	0.279	0.400	0.270	0.383
Advance coeff. J	0.202	0.316	0.201	0.312	0.193	0.295

Tab. 3. *Performance of the central propeller in the canal (propeller's diameter D = 1.100 m, and its rotational speed n = 345.2 rpm)*

Water depth h = 1.7 m						
Canal width b_0	9 m		20 m		50 m	
Ship speed V_S [m/s]	1.5	3.0	1.5	3.0	1.5	3.0
Nominal wake fraction w_n	0.185	0.341	0.156	0.307	0.073	0.212
Effective wake fraction w_e	0.717	0.535	0.662	0.490	0.529	0.371
Thrust coeff. K_T	0.459	0.407	0.456	0.402	0.448	0.384
Efficiency η	0.079	0.289	0.114	0.310	0.155	0.362
Advance coeff. J	0.068	0.289	0.081	0.247	0.112	0.302
Water depth h = 2.0 m						
Canal width b_0	9 m		20 m		50 m	
Ship speed V_S [m/s]	1.5	3.0	1.5	3.0	1.5	3.0
Nominal wake fraction w_n	0.437	0.402	0.469	0.419	0.564	0.529
Effective wake fraction w_e	0.020	0.234	0.043	0.245	0.117	0.348
Thrust coeff. K_T	0.393	0.330	0.416	0.365	0.421	0.381
Efficiency η	0.294	0.422	0.278	0.407	0.261	0.371
Advance coeff. J	0.232	0.362	0.226	0.362	0.208	0.314
Water depth h = 3.6 m						
Canal width b_0	9 m		20 m		50 m	
Ship speed V_S [m/s]	1.5	3.0	1.5	3.0	1.5	3.0
Nominal wake fraction w_n	0.165	0.161	0.185	0.181	0.223	0.219
Effective wake fraction w_e	- 0.220	0.005	- 0.204	0.221	- 0.172	0.056
Thrust coeff. K_T	0.366	0.278	0.396	0.337	0.399	0.340
Efficiency η	0.349	0.503	0.331	0.479	0.324	0.467
Advance coeff. J	0.288	0.470	0.284	0.463	0.277	0.446

Selected results are presented in Fig. 7 through 12.

The bottom pressure at the position where slope begins is presented in Fig. 7 and 8. At a lower water depth and lower canal width the destructive effect of moving ship over waterway bottom is stronger.

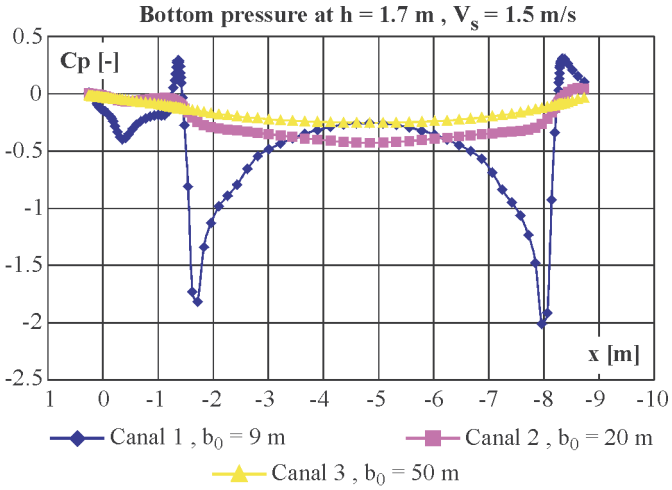

Fig.7. Longitudinal distribution of bottom pressure at the position where slope begins, for various values of canal width

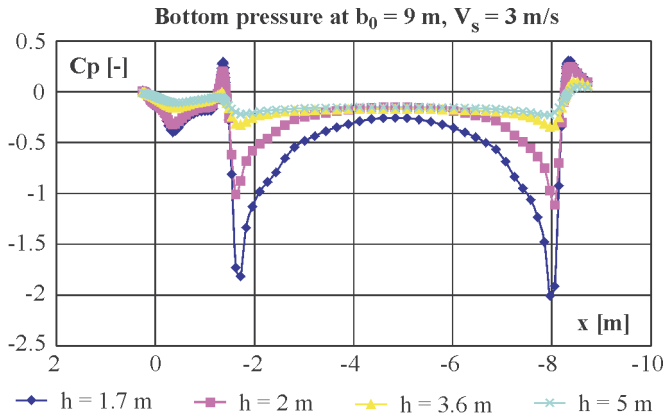

Fig.8. Longitudinal distribution of bottom pressure at the position where slope begins, for various values of water depth

The effect of canal width and water depth on performance of side propellers is presented in Fig. 9 through 12. The results show that the effect of banks is pronounced and depending on water depth. At the lowest depth h = 1.7 m the propeller thrust decreases when canal width increases. At the higher depths (h = 2.0 m and h = 3.6 m) the trend is opposite. An increase of water depth at a constant canal width causes a drop of propeller thrust. This effect can be explained by changes in water inflow to propeller that is reflected in variation of wake fraction.

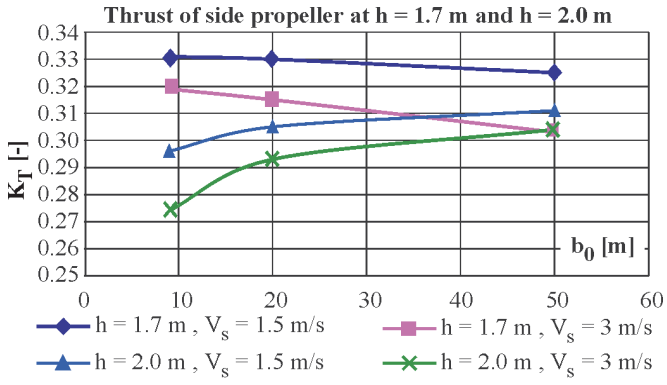

Fig.9. The effect of canal width on thrust generated by side propeller

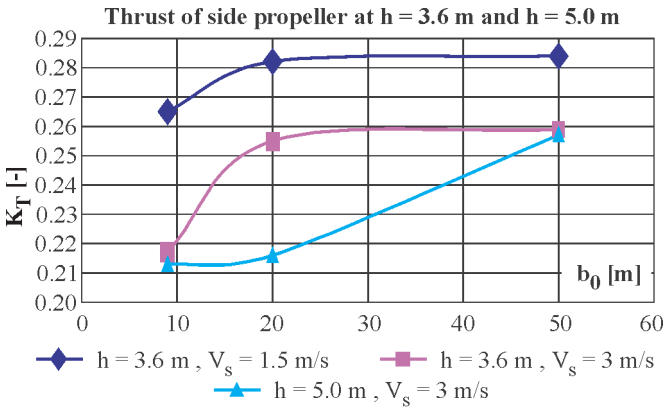

Fig.10. The effect of canal width on thrust generated by side propeller

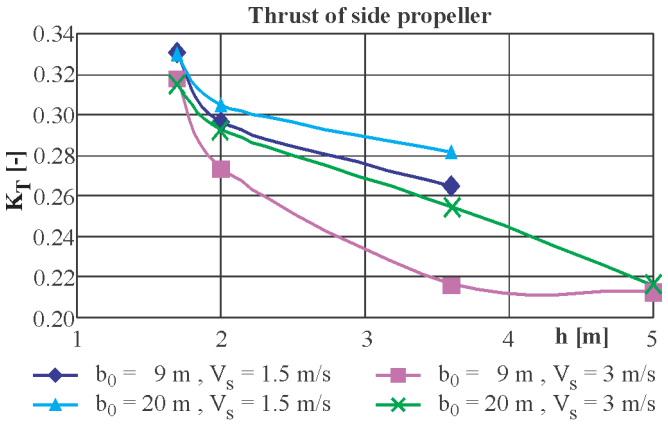

Fig.11. The effect of water depth on thrust generated by side propeller

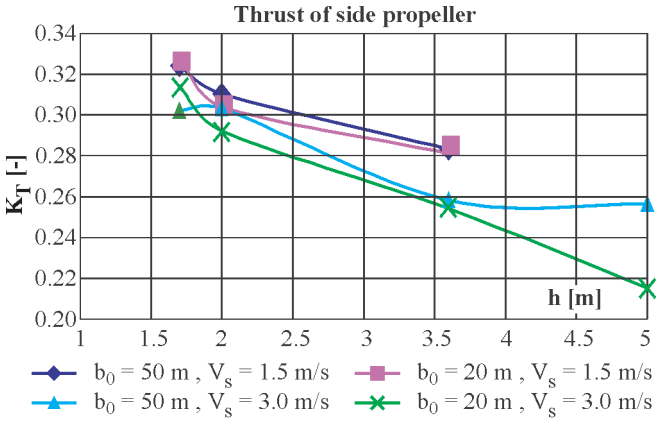

Fig.12. The effect of water depth on thrust generated by side propeller

In the case of the central propeller the effects of canal width and water depth are similar to those above presented.

If the ship is not positioned in the centreline of the canal the side propellers operate in different conditions. At the same rotational speed the starboard and portside propellers generate different thrust and the ship tends to turn if the turning moment is not compensated by rudders.

CONCLUSIONS

- It was proved that the applied computational method is a valuable tool to predict the performance of ducted propellers in shallow water, even at zero ship speed.
- Both the results of the model tests and computations reveal that the effect of water depth on thrust and pull at zero ship speed is insignificant.

- In the case of the considered barge train (d_b = 1.4 m and d_p = 0.6 m) the computed drop of bottom pressure beneath the running propeller is several times less than drop of pressure beneath bow and stern of barges. In general, it is the matter of ship and propeller arrangement as this factor leads to a greater destruction.

- The effect of canal banks and bottom on propeller performance in the case of the considered vessel is evident at the water depth below 3.6 m (h/d_b = 2.6 and h/d_p = 6.0) and the canal width below 20 m (b_0/B = 2.2). Propeller thrust at the lowest depth and width is 17% to 25% higher than that in wide and deep canal, depending on ship speed. Unfortunately the propeller efficiency drops then dramatically.

NOMENCLATURE

b_0 - canal width
B - moulded beam
c_P - pressure coefficient $(=\frac{P-P_{ref.}}{\frac{1}{2}\rho V_S^2})$
d - moulded draught
D - propeller diameter
h - water depth
J - advance coefficient
K_T - thrust coefficient $(=\frac{T}{\rho n^2 D^4})$
L_{OA} - overall length of ship
L_{WL} - length at waterline
n - rotational speed of propeller
P - local static pressure
$P_{ref.}$ - reference pressure (static pressure far upstream)
PS - plane of symetry
T - thrust of propeller
V_s - ship speed
w_e - effective wake fraction
w_n - nominal wake fraction
x - longitudinal co-ordinate, measured from propeller disc
η - propeller efficiency
ρ - water density
∇ - volumetric displacement

Indices

b - of barge
p - of pushboat

Acronyms

CFD - computational fluid dynamics
INBAT - innovative barge trains for effective transport on inland shallow waters
RTD - research and technological development

Acknowledgement

This research was financially supported by European Commission within the 5. Framework Programme (RTD project INBAT, contract No. G3RD-CT-2001-00458).

BIBLIOGRAPHY

1. Kulczyk J.: *Numerical modelling hydrodynamical effects in propulsion system of inland waterways ship* (in Polish), Prace Naukowe Instytutu Konstrukcji i Eksploatacji Maszyn Politechniki Wrocławskiej nr 66, Monografie nr 17 (Scientific Reports of the Institute of Machine Construction and Operation, Wrocław University of Technology). Wydawnictwo Politechniki Wrocławskiej (Publishing House of Wrocław University of Technology). Wrocław, 1992
2. Kulczyk J.: *Propeller-hull interaction in inland navigation vessel*, In: Marine Technology and Transportation (First International Conference on Marine Technology ODRA'95). Eds. T. Graczyk et al., Computational Mechanics Publ. Southampton, 1995
3. Skrzyński M.: *Open Water Propeller Tests,* Ship Design and Research Centre, Gdańsk (CTO) Report. Gdańsk, 2002
4. Skrzyński M.: *Bollard pull tests of pusher PBC1*, CTO Report. Gdańsk, 2003

CONTACT WITH THE AUTHORS

Wojciech Górski, M.Sc.,Eng.
Ship Design
and Research Centre S.A.
Wały Piastowskie 1
80-958 Gdańsk, POLAND
e-mail: wojciech.gorski@cto.gda.pl

Prof. Jan Kulczyk
Tomasz Tabaczek, D.Sc.,Eng.
Institute of Machine Design and Operation,
Wrocław University of Technology
Łukasiewicza 7/9
50-371 Wrocław, POLAND
e-mail: jan.kulczyk@pwr.wroc.pl
e-mail: tomasz.tabaczek@pwr.wroc.pl

Conference

A scientific seminar at Technical University of Koszalin

On 24 March 2005 the first-in- this-year scientific seminar of the Regional Group of the Section on Exploitation Foundations, Machine Building Committee, Polish Academy of Sciences, took place at the Department of Mechanical Engineering, Technical University of Koszalin.

According to the announced program of the seminar it was devoted to role of heuristics in didactic and scientific research activity. 4 papers on the topic were presented by scientific workers of the University, namely :

- *Heuristics in creative solving the educational problems* by J. Markul
- *Heuristics in innovation and development of products – – exemplified by a didactic task* – by J. Plichta
- *Heuristics as a method of solving logistic problems in manufacturing processes* – by G. Jurkowski
- *Heuristics applied to solve converse tasks in machine building* – by W. Tarnowski.

After interesting discussion the seminar's participants visited laboratories of the Department. Additionally, the hosts informed about very broad spectrum of didactic and scientific research lines of the Department's activity covering : mechanics and machine building, new technologies, solid body physics, materials engineering, optimization, automation, robotics and control, production process automation, mechatronics, data processing, modelling, simulation, artificial intelligence methods, biotechnologies, biochemistry, food processing, design, bionics.

An important form of the activity is the developing of cooperation with foreign scientific centres. In present the Department maintains contacts with three German and three French centres.

High-cycle fatigue criterion for anisotropic metals under multiaxial constant and periodic loads

Janusz Kolenda
Gdańsk University of Technology

ABSTRACT

Periodic stress with Cartesian components given in the form of Fourier series is considered. To account for the mean stress effect the modified Soderberg's formula is employed. An equivalent stress with synchronous components is defined. The design criterion for a finite fatigue life of metal elements is formulated. It covers the conditions of both static strength and fatigue safety in the high-cycle regime and includes material constants which have simple physical interpretation, can be determined by uniaxial tests, are related directly to the applied loads, and can reflect material anisotropy.

Key words : design criteria, multiaxial loading, periodic stress, mean stress effect

INTRODUCTION

In static problems, the load capacity of metal elements is referred to the yield strength and/or ultimate strength. In the case of multiaxial static loads, a reduced uniaxial stress, equivalent to the original one in terms of effort of the material, is taken into account. For ductile metals such stress model can be defined, for instance, with the aid of the Huber-von Mises-Hencky distortion-energy strength theory [1,2]. In the case of dynamic loading conditions, the design criteria of engineering elements made of ductile metals are frequently based on their fatigue limits and/or S-N curves (Wöhler curves) [3÷5] and, if the stress state is multiaxial and the stress components are proportional to each other, also on the distortion-energy theory [6,7]. In [8] the design criterion for an infinite fatigue life of metal elements under the stress with non-proportional components has been formulated with the aid of the average-distortion-energy strength hypothesis [9] and theory of energy transformation systems [10]. In this paper the design criteria for a finite fatigue life of metal elements under the stress with non-proportional components in the high-cycle regime are considered.

A CRITERION OF FINITE FATIGUE LIFE UNDER UNIAXIAL STRESS

If a metal element is subjected to an axial load producing the stress :

$$\sigma_a(t) = c + a \sin \omega t \tag{1}$$

where :

- a - stress amplitude
- c - mean value
- ω - circular frequency,

in design for an infinite fatigue life various „failure diagrams" or equations can be used [5,11]. For example, in [8] the Soderberg's equation has been utilized. Its necessary modification to indicate finite fatigue lives resulted in the following formula [11] :

$$a = \sigma (1 - c/R_e) \tag{2}$$

where :

- R_e - tensile yield strength
- σ - amplitude of the fully reversed stress at a given number, N, of cycles to failure
- a - amplitude of the stress (1) which leads to that fatigue life.

For the relation between σ and N in the high-cycle fatigue regime the following equation of the S - N curve is commonly accepted :

$$N\sigma^m = K \tag{3}$$

where :

- K - fatigue strength coefficient
- m - fatigue strength exponent.

Introducing the safety factor :

$$f = \frac{N}{N_d} = \frac{T}{T_d} \tag{4}$$

where :

- $N_d = \omega T_d /(2\pi)$ - required number of stress cycles to achieve a given design life T_d
- T - time to failure under the stress (1)

and partial safety factors :

$$f_d = \frac{N_a}{N_d} \qquad f_s = \frac{R_e}{c} \tag{5}$$

where :

$$N_a = \frac{K}{a^m} \tag{6}$$

one gets

$$f = f_d(1 - f_s^{-1})^m \tag{7}$$

The criterion in question reads :

$$f \geq 1 \tag{8}$$

that is :

$$f_d(1 - f_s^{-1})^m \geq 1 \tag{9}$$

Eq. (9) can be rewritten as :

$$f_d^{-1/m} + f_s^{-1} \leq 1 \tag{10}$$

i.e.,

$$\left(\frac{N_d}{K}\right)^{1/m} a + \frac{1}{R_e} c \leq 1 \tag{11}$$

It is seen that Eq.(11) covers both the condition of static strength and the fatigue safety requirement. This advantage will be maintained in what follows. To be on the safe side, in the case of $c < 0$ it is recommended to insert into Eq. (11) the compressive yield strength $R_{ec} < 0$ in place of R_e .

A CRITERION OF FINITE FATIGUE LIFE UNDER OUT-OF-PHASE STRESS

On the basis of the average-distortion-energy strength hypothesis [9], the stress with Cartesian components :

$$\sigma_i(t) = c_i + a_i \sin(\omega t + \beta_i) \tag{12}$$

$$i = x, y, z, xy, yz, zx$$

can be modelled by the reduced stress [12] :

$$\sigma_{eq}(t) = c_{eq} + a_{eq} \sin \omega t \tag{13}$$

equivalent in terms of effort of the material under the stress with the components (12), where :

c_i , a_i , β_i - mean value, amplitude and phase angle of i-th stress component, respectively

c_{eq} , a_{eq} - mean value and amplitude of the reduced stress, given by (for the sake of brevity the stress components σ_z , σ_{yz} and σ_{zx} have been dropped)

$$c_{eq} = (c_x^2 + c_y^2 - c_x c_y + 3c_{xy}^2)^{1/2} \tag{14}$$

$$a_{eq} = [a_x^2 + a_y^2 - a_x a_y \cos(\beta_x - \beta_y) + 3a_{xy}^2]^{1/2} \tag{15}$$

Consequently, the criterion (11) becomes :

$$\left(\frac{N_d}{K}\right)^{1/m} a_{eq} + \frac{1}{R_e} c_{eq} \leq 1 \tag{16}$$

or, in explicit form

$$\left(\frac{N_d}{K}\right)^{1/m} [a_x^2 + a_y^2 - a_x a_y \cos(\beta_x - \beta_y) + 3a_{xy}^2]^{1/2} + \frac{1}{R_e}(c_x^2 + c_y^2 - c_x c_y + 3c_{xy}^2)^{1/2} \leq 1 \tag{17}$$

In particular, the criterion (17) may be useful for isotropic steels where [1] :

$$R_{es} = \frac{1}{\sqrt{3}} R_e \qquad F_t = \frac{1}{\sqrt{3}} F_b \tag{18}$$

where :

R_{es} - shear yield strength

F_b - fatigue limit under fully reversed bending

F_t - fatigue limit under fully reversed torsion.

With Eqs (18), the criterion of finite fatigue life for steel elements under out-of-phase stress can be also expressed as :

$$\left(\frac{N_d}{K}\right)^{1/m} [a_x^2 + a_y^2 - a_x a_y \cos(\beta_x - \beta_y) + \left(\frac{F_b}{F_t}\right)^2 a_{xy}^2]^{1/2} + \frac{1}{R_e}[c_x^2 + c_y^2 - c_x c_y + \left(\frac{R_e}{R_{es}}\right)^2 c_{xy}^2]^{1/2} \leq 1 \tag{19}$$

A CRITERION OF FINITE FATIGUE LIFE UNDER OUT-OF-PHASE STRESS FOR ANISOTROPIC METALS

Metals may be isotropic or anisotropic with respect to any type of behaviour, such as thermal conductivity, electrical resistivity, thermal expansion, plastic deformation, or fatigue strength. This paper is concerned with differences in yield strengths and fatigue limits in different directions as well as under loads of different modes. For instance, uniform stress field under axial load versus nonuniform one under bending contributes to significant difference in the relevant fatigue limits.

Anisotropy can be introduced by cold-working operations such as rolling, forging, drawing or stretching. For example, even small amounts of strain can cause a considerable difference in the longitudinal and transverse yield strengths. In other words, as a result of the longitudinal prestrain the tensile and compressive yield strengths are different in the transverse direction, as well as in longitudinal direction, though to a smaller degree [13]. Cold rolling of a wide plate and cold drawing of a tube over a mandrel both result in a lengthening and thinning, with no change in the transverse dimension (width or diameter), and so the resulting anisotropy is similar in the two products. In both cases, the anisotropy exhibits three mutually perpendicular planes of symmetry. In drawing of a rod (or tubing without a mandrel), the two transverse strains are equal, and so the anisotropy reveals an axis of symmetry.

For different metals and different fabrication methods the degree of anisotropy varies within wide limits; some metals are so nearly isotropic that it may be difficult to detect a difference in properties in different directions, such as in the case of the yield strengths in the normal and rolling directions of hot-rolled mild-steel plate; however other metals may be highly anisotropic.

In order to take into account the material anisotropy and load modes, in this paper the following modification of Eq. (19) is suggested :

$$\left(\frac{N_d}{K}\right)^{1/m}\left[\left(\frac{F_b}{F_x}a_x\right)^2+\left(\frac{F_b}{F_y}a_y\right)^2-\left(\frac{F_b}{F_x}a_x\right)\left(\frac{F_b}{F_y}a_y\right)\cos(\beta_x-\beta_y)+\left(\frac{F_b}{F_t}\right)^2\left(\frac{F_t}{F_{xy}}a_{xy}\right)^2\right]^{1/2}+$$
$$+\frac{1}{R_e}\left[\left(\frac{R_e}{R_x}c_x\right)^2+\left(\frac{R_e}{R_y}c_y\right)^2-\left(\frac{R_e}{R_x}c_x\right)\left(\frac{R_e}{R_y}c_y\right)+\left(\frac{R_e}{R_{es}}\right)^2\left(\frac{R_{es}}{R_{xy}}c_{xy}\right)^2\right]^{1/2}\le 1 \tag{20}$$

where :

F_x - fatigue limit under fully reversed load relevant to the normal stress component of the amplitude a_x
F_{xy} - fatigue limit under fully reversed load associated with the shear stress component of the amplitude a_{xy}
R_x - absolute value of the yield strength relevant to the constant load inducing the normal stress component c_x
R_{xy} - yield strength associated with the constant load giving the shear stress component c_{xy} .

The remaining material constants R_i and F_i are defined analogously.

Eq. (20) yields the requested criterion :

$$\left(\frac{N_d}{K}\right)^{1/m}F_b\left[\sum_i\left(\frac{a_i}{F_i}\right)^2-\frac{a_xa_y}{F_xF_y}\cos(\beta_x-\beta_y)\right]^{1/2}+\left[\sum_i\left(\frac{c_i}{R_i}\right)^2-\frac{c_xc_y}{R_xR_y}\right]^{1/2}\le 1 \tag{21}$$

A CRITERION OF FINITE FATIGUE LIFE UNDER MULTIAXIAL CONSTANT AND PERIODIC STRESSES FOR ANISOTROPIC METALS

Let us consider a periodic stress with Cartesian components given by Fourier series :

$$\sigma_i(t)=c_i+\sum_{p=1}^{\infty}a_{ip}\sin(p\omega_o t+\beta_{ip}) \qquad i=x,\,y,\,xy \tag{22}$$

where :

c_i - mean value of i-th stress component
a_{ip} , β_{ip} - amplitude and phase angle of p-th term in Fourier expansion of i-th stress component
$\omega_0 = 2\pi/T_0$ - fundamental circular frequency
T_0 - common period of the stress components.

Following the results obtained in [8] and [12], the stress components (22) are modelled by the equivalent stress components :

$$\sigma_i^{(eq)}(t)=c_i^{(eq)}+a_i^{(eq)}\sin(\omega_{eq}t+\varphi_i) \qquad i=x,\,y,\,xy \tag{23}$$

where [8] :

$$c_i^{(eq)}=c_i \qquad a_i^{(eq)}=\left(\sum_{p=1}^{\infty}a_{ip}^2\right)^{1/2} \qquad a_x^{(eq)}a_y^{(eq)}\cos(\varphi_x-\varphi_y)=\sum_{p=1}^{\infty}a_{xp}a_{yp}\cos(\beta_{xp}-\beta_{yp}) \tag{24}$$

and [12] :

$$\omega_{eq}=k\omega_0 \qquad k=\mathrm{Round}(\kappa) \tag{25}$$

$$\kappa=\left[\frac{\sum_{p=1}^{\infty}(pa_{xp})^2+\sum_{p=1}^{\infty}(pa_{yp})^2-\sum_{p=1}^{\infty}p^2a_{xp}a_{yp}\cos(\beta_{xp}-\beta_{yp})+3\sum_{p=1}^{\infty}(pa_{xyp})^2}{\sum_{p=1}^{\infty}a_{xp}^2+\sum_{p=1}^{\infty}a_{yp}^2-\sum_{p=1}^{\infty}a_{xp}a_{yp}\cos(\beta_{xp}-\beta_{yp})+3\sum_{p=1}^{\infty}a_{xyp}^2}\right]^{1/2} \tag{26}$$

Here k is a natural number, φ_i, is the phase angle of i-th equivalent stress component and ω_{eq} is the equivalent circular frequency. Eq. (26) has been derived by means of the theory of energy transformation systems [10] under assumption that the material is ductile and isotropic. Its modification for ductile and isotropic materials, similar to that of Eq. (17), leads to :

$$\kappa=\left[\frac{\sum_i\sum_{p=1}^{\infty}\left(\frac{pa_{ip}}{F_i}\right)^2-\sum_{p=1}^{\infty}\frac{a_{xp}a_{yp}}{F_xF_y}p^2\cos(\beta_{xp}-\beta_{yp})}{\sum_i\sum_{p=1}^{\infty}\left(\frac{a_{ip}}{F_i}\right)^2-\sum_{p=1}^{\infty}\frac{a_{xp}a_{yp}}{F_xF_y}\cos(\beta_{xp}-\beta_{yp})}\right]^{1/2} \tag{27}$$

Adaptation of Eq. (21) to the equivalent stress with the components (23) gives :

$$\left(\frac{N_d}{K}\right)^{1/m} F_b\left[\sum_i\left(\frac{a_i^{(eq)}}{F_i}\right)^2 - \frac{a_x^{(eq)}a_y^{(eq)}}{F_xF_y}\cos(\varphi_x-\varphi_y)\right]^{1/2} + \left[\sum_i\left(\frac{c_i^{(eq)}}{R_i}\right)^2 - \frac{c_x^{(eq)}c_y^{(eq)}}{R_xR_y}\right]^{1/2} \le 1 \tag{28}$$

where :

$$N_d = \frac{\omega_{eq}T_d}{2\pi} \tag{29}$$

Hence the criterion of finite fatigue life for engineering details made of anisotropic ductile materials and subjected to multiaxial constant and periodic loads becomes :

$$\left(\frac{\omega_{eq}T_d}{2\pi K}\right)^{1/m} F_b\left[\sum_i\sum_{p=1}^{\infty}\left(\frac{a_{ip}}{F_i}\right)^2 - \frac{1}{F_xF_y}\sum_{p=1}^{\infty}a_{xp}a_{yp}\cos(\beta_x-\beta_y)\right]^{1/2} + \left[\sum_i\left(\frac{c_i}{R_i}\right)^2 - \frac{c_xc_y}{R_xR_y}\right]^{1/2} \le 1 \tag{30}$$

EXAMPLE

Assumptions

Suppose the stress components and material data (in MPa) are :

$\sigma_x(t) = c_x + a_x \sin\omega t$ – normal stress component

$\sigma_{xy}(t) = c_{xy} + a_{xy}\sin\omega t$ – shear stress component

$c_x = 50 \quad a_x = 90 \quad c_{xy} = 40 \quad a_{xy} = 60$

$R_e = 260 (\text{steel } 25) \quad R_{es} = 160$

$R_{eg} = 310$ – yield strength in bending

$F_b = Z_{go} = 180 \quad F_t = Z_{so} = 110$

$F_x = Z_{rc} = 150$ – fatigue limit under fully reversed tension - compression.

Task

Compare the criteria (17) and (21) in the following cases :

A. the normal stress component is caused by bending moment
B. the normal stress component is caused by axial force.

Solution

A common and conservative strategy in classical fatigue design for applying the distortion-energy strength theory is to separately compute the equivalent stress corresponding to the mean stress and the equivalent stress corresponding to the amplitude [14]. Similar results have been obtained with the aid of the average - distortion - energy strength hypothesis, Eqs. (14) and (15), which will be used in the considered Example.

A. Eqs (14) and (15) yield :

$$c_{eq} = (c_x^2 + 3c_{xy}^2)^{1/2} = (50^2 + 3\cdot 40^2)^{1/2} = 85.44\,\text{MPa}$$

$$a_{eq} = (a_x^2 + 3a_{xy}^2)^{1/2} = (90^2 + 3\cdot 60^2)^{1/2} = 137.48\,\text{MPa}$$

So, Eq. (17) becomes :

$$137.48\left(\frac{N_d}{K}\right)^{1/m} + \frac{85.44}{260} \le 1$$

Hence :

$$\left(\frac{N_d}{K}\right)^{1/m} \le 48.83\cdot 10^{-4}$$

With Eq. (21) one obtains :

$$\left(\frac{N_d}{K}\right)^{1/m} 180\left(\frac{90^2}{180^2} + \frac{60^2}{110^2}\right)^{1/2} + \left(\frac{50^2}{310^2} + \frac{40^2}{160^2}\right)^{1/2} \le 1$$

i.e.,

$$\left(\frac{N_d}{K}\right)^{1/m} \le 52.74\cdot 10^{-4}$$

B. In this case Eq. (17) leads to the same results as with the bending stress, that is :

$$\left(\frac{N_d}{K}\right)^{1/m} \le 48.83\cdot 10^{-4}$$

whereas Eq. (21) gives :

$$\left(\frac{N_d}{K}\right)^{1/m} 180\left(\frac{90^2}{150^2} + \frac{60^2}{110^2}\right)^{1/2} + \left(\frac{50^2}{260^2} + \frac{40^2}{160^2}\right)^{1/2} \le 1$$

$$\left(\frac{N_d}{K}\right)^{1/m} \le 46.90\cdot 10^{-4}$$

The differences between these results are self-explanatory.

CONCLUSIONS

- The finite fatigue life design criterion covering the conditions of both static strength and fatigue safety of metal elements under multiaxial constant and periodic loads, has been formulated.
- The presented criterion includes material constants which
  - ⇨ have simple physical interpretation
  - ⇨ can be determined by uniaxial tests
  - ⇨ are directly related to the applied load
  - ⇨ can reflect material anisotropy.
- Similarly as in vibration problems, it is not possible to state a definite upper limit to *p* in (22), (24), (26), (27) and (30), since this depends upon the nature and origin of the considered stress variations, as well as upon the influence of minor terms on fatigue endurance of various materials, which may be the source of uncertainties.

NOMENCLATURE

- a - stress amplitude
- a_i - amplitude of i-th stress component (i = x, y, z, xy, yz, zx)
- a_{eq} - amplitude of the reduced stress
- a_{ip} - amplitude of p-th term in Fourier expansion of i-th stress component
- $a_i^{(eq)}$ - amplitude of i-th component of the equivalent stress
- c - mean stress value
- c_i - mean value of i-th stress component
- c_{eq} - mean value of the reduced stress
- $c_i^{(eq)}$ - mean value of i-th component of the equivalent stress
- f - safety factor
- f_d , f_s - partial safety factors
- F_b , F_t - fatigue limits under fully reversed bending and torsion, respectively
- F_i - fatigue limit under fully reversed load associated with the stress component of the amplitude a_i
- k - natural number obtained by rounding the number κ
- K - fatigue strength coefficient in equation of the S-N curve for tension-compression
- m - fatigue strength exponent in equation of the S-N curve for tension- compression
- N , N_a - numbers of zero mean stress cycles to cause failure at the stress amplitudes σ and a, respectively
- N_d - required number of stress cycles to achieve a given design life
- R_e , R_{es} - tensile and shear yield strengths, respectively
- R_i - yield strength associated with the constant load inducing the stress component c_i
- t - time
- T - time to fatigue failure
- T_d - design life
- T_0 - stress period
- β_i - phase angle of i-th stress component
- β_{ip} - phase angle of p-th term in Fourier expansion of i-th stress component
- κ - quantity given by Eq. (27)
- σ - stress amplitude satisfying Eq. (3)
- σ_a - stress produced by axial load
- σ_i - i-th stress component
- σ_{eq} - reduced stress
- $\sigma_i^{(eq)}$ - i-th component of the equivalent stress
- φ_i - phase angle of i-th component of the equivalent stress
- ω - circular frequency
- ω_0 - fundamental circular frequency of the periodic stress
- ω_{eq} - equivalent circular frequency

BIBLIOGRAPHY

1. Blake A. (Ed.): *Handbook of mechanics, materials and structures*. J. Wiley & Sons. New York, 1985
2. Życzkowski M. (Ed.): *Technical mechanics. Vol. 9, Strength of structural elements* (in Polish). PWN (Scientific Work Publishers). Warszawa, 1988
3. Osgood C.C.: *Fatigue design.* Pergamon Press. Oxford, 1982
4. Troshchenko V.T., Sosnovskii L.A.: *Fatigue strength of metals and alloys* (in Russian). Naukowa Dumka. Kiev, 1987
5. Kocańda S., Szala J.: *Fundamentals of fatigue calculations* (in Polish). PWN. Warszawa, 1997
6. Troost A., E1-Magd E.: *Schwingfestigkeit bei mehrachsiger Beanspruchung ohne und mit Phasenverschiebung.* Konstruktion, No 8/1981
7. Sonsino C.M.: *Multiaxial fatigue of welded joints under in-phase and out-of-phase local strains and stresses.* Int. Journal Fatigue, No 1/1995
8. Kolenda J.: *Fatigue "safe-life" criterion for metal elements under multiaxial constant and periodic loads.* Polish Maritime Research, No 2/2004
9. Kolenda J.: *Average-distortion-energy strength hypothesis.* Proc. of 17th Symp. on Fatigue and Fracture Mechanics. Bydgoszcz--Pieczyska, 1998. Academy of Agriculture & Engineering. Bydgoszcz, 1998
10. Cempel C.: *Theory of energy transformation systems and their application in diagnostic of operating systems.* Applied Math. and Computer Sciences, No 3/1993
11. Almar-Naess (Ed.): *Fatigue handbook. Offshore steel structures.* Tapir Publishers. Trondheim, 1985
12. Kolenda J.: *On fatigue safety of metallic elements under static and dynamic loads.* Gdańsk University of Technology Publishers. 2004
13. Lubahn J.D., Felgar R.P.: *Plasticity and creep of metals.* J. Wiley & Sons. New York, London, 1961
14. Haslach H.W., Jr, Armstrong R.W.: *Deformable bodies and their material behavior.* J.Wiley & Sons. 2004

CONTACT WITH THE AUTHOR

Prof. Janusz Kolenda
Faculty of Ocean Engineering
and Ship Technology,
Gdańsk University of Technology
Narutowicza 11/12
80-952 Gdańsk, POLAND
e-mail : sek7oce@pg.gda.pl

Conference

Safety at sea and marine environment protection

These were the topics of 9th Technical Scientific Conference held in Kołobrzeg on Baltic Sea coast on 2 ÷ 3 June 2005. The conference program contained 17 papers presented during two sessions :

Safety of navigation and rescue of lives at sea (13 papers)
Marine environment protection (4 papers).

Out of the presented topics, 8 papers dealt with local problems, and general ones were given in the following papers :

- *Safety of maritime turism in the polar regions, with Antarctica as an example* – by J. Frydecki and A. Wolski (Martime University of Szczecin)
- *Development trends in modelling the areas of search at sea* – by Z. Burciu (Gdynia Maritime University)
- *Contemporary methods for classification of free- drift phenomenon* – by M. Drogosiewicz and A. Wójcik (Polish Naval University)
- *Problems associated with dynamical determining the search area* – by T. Budny (Gdynia Maritime University)
- *Introduction of manoeuvrability standards in the low--speed range as an element of improvement of port operation safety* – by T. Abramowicz-Gerigk (Gdynia Maritime University)
- *Modelling the life- raft sinkage probability* by L. Smolarek (Gdynia Maritime University)
- *Probability of radar detection of rigid inflatable boats (RIB) fitted with active radar reflectors* – by A . Szklarski (Gdynia Maritime University)
- *Application of ultrafiltration technique to bilge water purification* – by Z. Jóźwiak and A. Kozłowski (Maritime University of Szczecin)
- *Research on deoiling process of oil/water emulsion by means of ceramic bulkheads* – by J. M. Gutteter – Grudziński (Maritime University of Szczecin).

Forces exciting vibrations of ship's hull and superstructure

Lech Murawski
Ship Design and Research Centre, Gdańsk

ABSTRACT

The paper presents identification of main excitation forces of vibrations of ship hull and its superstructure, as well as investigation of influence of the analyzed excitation on ship vibration level. The following excitation forces were analyzed: dynamic pressure on the transom deck, propeller-generated hydrodynamic forces, as well as internal and external engine-generated forces. Rigidity and attenuation characteristics of lubricating oil film were taken into account in the analysis of the excitations transmitted by the propulsion system bearings (stern tube bearing, intermediate bearing, engine's main and thrust bearings). The dynamic characteristics of ship's power transmission system were also taken into account. Results of the analyzes were verified by comparing results of the computations and measurements.

Keywords : hull vibration, superstructure vibration, main engine vibrations, excitation forces, pressure pulses, propulsion system's reactions, crankshaft-propeller phasing

INTRODUCTION

The following main forces exciting vibrations of ship hull and superstructure (Fig.1) were considered [1,12] :

1. propeller-induced pressure pulses upon the ship transom deck
2. dynamic reactions of the thrust bearing to non-coupled longitudinal vibration of the power transmission system (generated by axial hydrodynamic force of the propeller)
3. dynamic reactions of the thrust bearing to coupled longitudinal vibration of the power transmission system (generated by kinematic couplings of the crankshaft and hydrodynamic couplings of the propeller)
4. dynamic reactions of the radial bearings (stern tube bearing, intermediate bearings and main bearings of the engine), generated by hydrodynamic radial forces and moments induced on the propeller
5. non-balanced moments of the main engine, generated by gas and inertia forces of piston-crank system.

The analysis was performed for the cargo ships (mainly for medium size containers) with typical propulsion system – a constant pitch propeller directly driven by a low speed main engine. In the paper an example analysis was made for a 2700 TEU container carrier. The ship particulars were as follows: ship length – 207 m, maximum deadweight – 35600 t, speed – – 22.7 knots. The ship was powered by MAN B&W 8S70MC-C engine of 24840 kW rated output at 91 rpm. The five-blade propeller was of 7.6 m diameter and 42400 kg in weight. All conclusions are valid for the ship loaded with containers from 1200 TEU up to 4500 TEU in number. For the analysis of the ship's hull and superstructure vibrations Patran-Nastran software was used, whereas the analysis of excitation forces (dynamic calculations of the power transmission system) was made mainly with the use of the author's DSLW FEM – based software dealing with coupled torsional-bending-longitudinal vibrations of power transmission system [7] and DRG one concerning shaft line whirling vibrations [8].

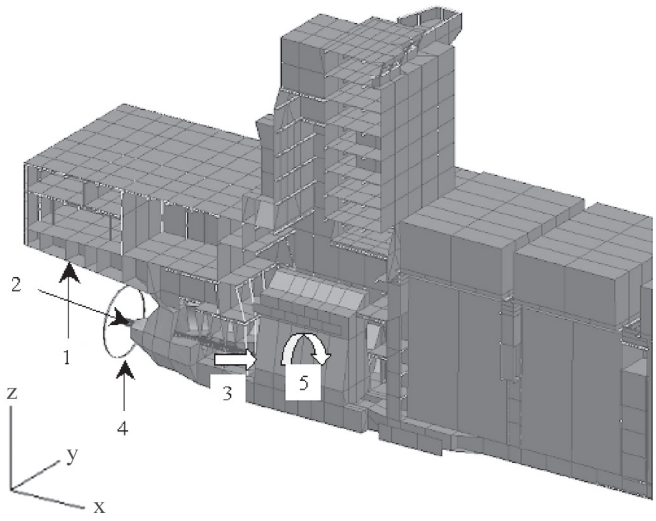

Fig. 1. *Excitation forces of ship's hull and superstructure vibrations*

Reactions of stern bearing, shaft line bearing and main bearings of the engine are generated by bending vibration of the shaftline. The reaction level and distribution depend on shaft line alignment [5,11] and on stiffness-damping characteristics of lubricating oil film in the bearings [6,8]. The stiffness-damping characteristics of the oil film were found with the use of the author's BRG software based on Finite Difference Method [6]. Dynamic rigidities of ship hull structure within areas of bearing foundations were determined with the use of Nastran software.

Analysis of bending vibration of the propeller shaftline showed a low level of bending vibration, nevertheless the level of dynamic reactions of the bearings (particularly the stern tube bearing) was significant. It may be a source of excessive vibrations of ship hull and superstructure.

Reactions of the thrust bearing are generated by longitudinal vibration of the power transmission system. [3,7]. Two basic sources of longitudinal vibration excitation forces may be distinguished : excitations generated by the main engine [4,7] (coupled torsional-bending-longitudinal vibrations) and excitations generated by the propeller (coupled and non-coupled hydrodynamic forces). During the analysis total reactions of the thrust bearing, generated by all kinds of kinematic couplings were found. These reactions result from longitudinal vibrations of the power transmission system, coupled with torsional-bending vibrations [3,7]. Non-linear characteristics of thrust bearing's oil film were taken into account during the calculation.

Reaction phases generated by non-coupled vibrations were determined with respect to propeller blade (phase „zero" was assumed for the upper position of the blade). Reaction phases generated by coupled vibrations were determined with respect to the first crank of the engine (phase „zero" was assumed for the top dead centre). The amount of total reactions (generated by coupled and non-coupled vibrations) depends on mutual phasing of propeller blades and crankshaft. With a suitable arrangement of angular position of the propeller (in relation to the crankshaft) the resultant vector of the reactions can be reduced to algebraic difference of modules of the summed reactions. The optimum setting angle of the propeller with respect to main engine cranks depends on rotational speed of the propulsion system, minimized harmonic component and load condition of the ship.

The reaction of longitudinal vibration damper should be applied to the axis of the crankshaft due to its full symmetry. To find the application point of thrust bearing reaction is more difficult. The thrust bearing (of Mitchell type) consists of pads supported at their edges and arranged at the perimeter of thrust disk. Generally the pads do not fill completely the full perimeter, being installed at the lower part of the thrust disk. In this case the axis of thrust bearing reaction should be lowered. Another solution consists in applying the thrust bearing reaction in line with the crankshaft axis and adding a suitable bending moment as a transverse dislocation of force does not change the loading system if adequate moment is added. The effect of neglecting this moment on the vibration level of ship hull and its superstructure should be investigated during further numerical analysis.

Regardless of the bearing forces, vibrations of ship hull and its superstructure are generated by pressure pulses induced on the plating above the propeller (transom), as well as by unbalanced internal forces of the main engine. The pressures, their distribution and phase shift are specified by designers of the propeller. The unbalanced forces and moments of the main engine are the last significant forces to be analyzed. In contemporary main engines all the external forces are generally balanced. The remaining moments which excite the following vibrations of engine body, should be investigated: vertical-longitudinal (ML), vertical-horizontal (MH) and torsional vibrations around the vertical axis (MX). For the engine in question, (i.e. MAN B&W 8S70MC-C), only the 1^{st}, 3^{rd},4^{th}, 5^{th} and 8^{th} harmonic components of excitations are significant from the point of view of ship hull and superstructure vibrations.

Two main structural models of the 2700 TEU container carrier were used for the computations :

- the model for the ship in the design load condition (Fig.2)
- and that for the ship in the ballast condition [9,10].

Each of the models contained more than 42000 degrees of freedom.

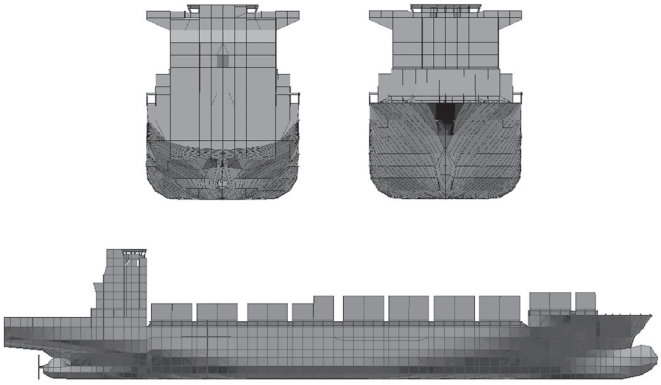

Fig. 2. *Structural model of 2700 TEU container carrier in the design load condition*

Results of the computations are presented for the representative group of the points (all the points, except the bridge wings, are placed in the ship plane of symmetry) located as follows :

- ⇨ **BOW** – at hull bow on the main deck
- ⇨ **DTR** – at deck transom edge on the main deck
- ⇨ **SBF** – at fore bottom of the superstructure
- ⇨ **SBB** – at aft bottom of the superstructure
- ⇨ **MEF** – at main engine fore cylinder heads
- ⇨ **MEB** – at main engine aft cylinder heads
- ⇨ **STL** – at bridge wing (left)
- ⇨ **STF** – at fore top of the superstructure
- ⇨ **STB** – at aft top of the superstructure

KINDS OF EXCITATION

The analyses of forced vibrations were made for the container carrier in the design load condition (Fig. 1) without added mass of water. The wet model of ship hull was used to find the total forced vibrations (generated by complex sources of excitations) and to compare them with measurement results. Computations for the container carrier in the ballast condition were also carried out because it was the condition of the ship during the measurements.

The propeller induces a variable field of water pressure exciting vibration of ship transom deck. The vibrations are transmitted to all parts of the ship structure. Vibrations excited by the first-blade (5^{th} harmonic) component of propeller-induced excitations were analyzed. The image of forced vibration velocities of the ship hull, superstructure and main engine is shown in Fig.3.

Hydrodynamic forces and moments are induced by rotating propeller. Only the variable hydrodynamic forces acting in line with propeller shaft and generating non-coupled axial vibration of the propulsion system are discussed. Phases of these vibrations are strictly associated with the propeller. The non-coupled axial vibrations of the power transmission system generate excitations to ship hull and superstructure through the

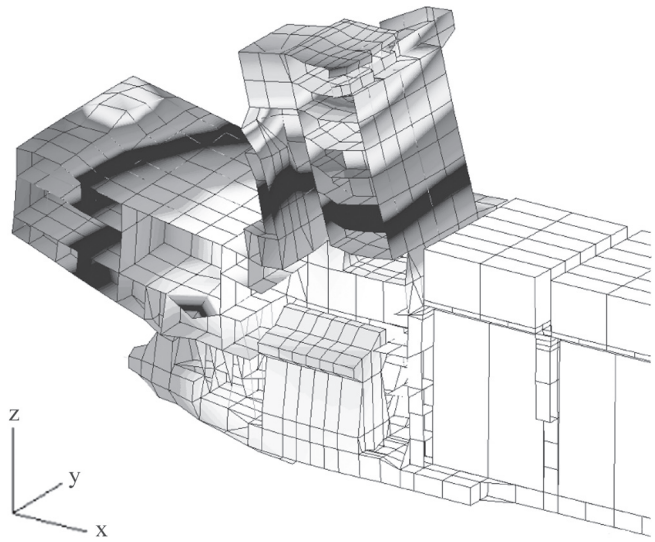

Fig. 3. *Vibration velocities of the container carrier, excited by water pressure field on the transom deck*

thrust bearing and axial vibration damper. The forced vibration of ship hull, superstructure and main engine is presented in Fig.4.

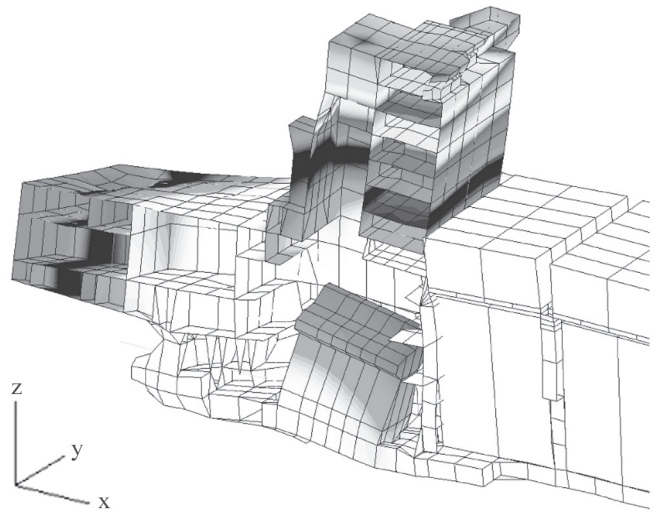

Fig. 4. *Vibration velocities of the container carrier, forced by axial vibrations of its propulsion system*

Torsional-bending vibrations are generated by ship propulsion system. Bending of crankshaft cranks and torsional vibrations of the crankshaft and propeller generate coupled longitudinal vibrations of the power transmission system. The longitudinal vibrations induce dynamic reactions on the thrust bearing and axial vibration damper, generating excitations to ship hull and superstructure. Phases of the coupled longitudinal vibrations depend mainly on the position of main engine crankshaft.

The coupled longitudinal vibrations are mainly due to gas and inertia forces generated in the engine cylinders. Therefore a relatively wide spectrum of harmonic components may be of significant importance. In the considered case the first eight harmonic reactions (8-cylinder engine) are significant. Therefore eight variants of computation of the forced vibrations of ship hull and superstructure were carried out, i.e. for all significant harmonic components of exciting forces. Distribution of forced vibration velocities for the ship is similar to that shown in Fig.4.

The general image of forced vibration amplitudes (velocities) for all the considered harmonic components is shown in Fig.5.

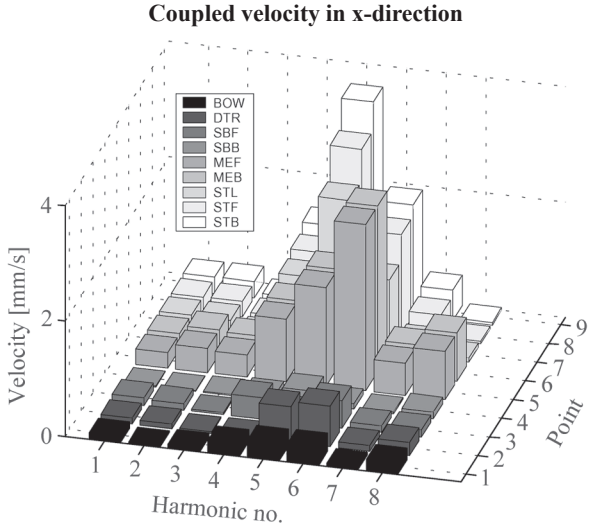

Fig. 5. *Longitudinal vibration velocities forced by coupled longitudinal vibrations*

As in the case of other kind of exciting forces, the highest vibration level appears in the upper part of ship superstructure. The 5^{th} harmonic component is dominant as in the case of excitations generated by the propeller. The levels of expected vibrations generated by the coupled and non-coupled longitudinal vibrations of the propulsion system are similar. Phases of vibrations generated by the non-coupled vibrations depend on a position of the propeller blades, whereas phases of vibrations generated by the coupled vibrations depend on a position of the crankshaft cranks. Therefore a mutual angular position of the propeller and crankshaft may significantly affect vibration level of ship superstructure. This problem is further investigated below. Side harmonic components (with respect to 5^{th} component), i.e. 6^{th} and 4^{th} components may be dominating for vibrations of the main engine body and ship hull.

The transverse forces and moments induced by rotating propeller generate bending vibration of the shaftline. The bending vibrations generate dynamic reactions of radial bearings of the propulsion system, i.e. the stern tube bearing, intermediate bearing and main bearings of the main engine. The resulting bending vibrations of the shaftline generate forced vibration of ship hull and superstructure.

Fig.6 presents the vibration velocities of ship hull, superstructure and main engine, forced by transverse vibration of the propulsion system.

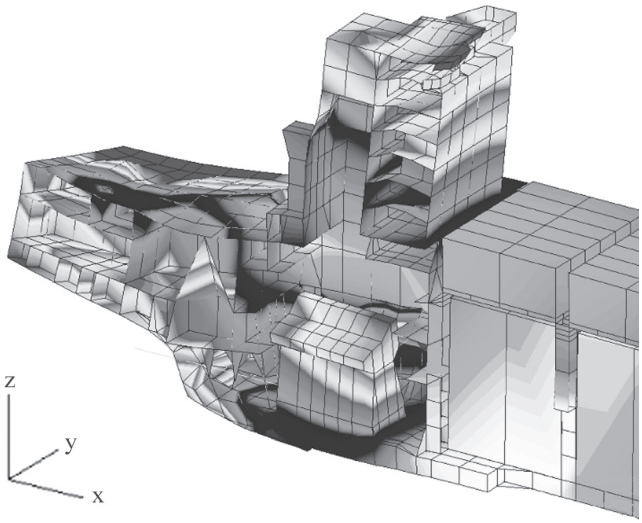

Fig. 6. *Vibration velocities of the container carrier, forced by transverse vibration of the propulsion system*

Non-balanced external dynamic forces and moments appear as a result of operation principle of piston engines. In ship engines all external forces and high-order moments are balanced. However some of the moments remain still non-balanced. The moments generate longitudinal, transverse and torsional vibrations of the engine, transmitted to other structural parts of the ship. Values of the non-balanced moments are given in the engine documentation. For the considered engine the following harmonic components are significant: 1, 3, 4, 5, and 8.

Velocities of forced vibrations of the ship for: 1st harmonic (excitation of L and X type), 3rd harmonic (excitation of X type), 5th harmonic (excitation of X type) and 8th harmonic component (excitation of H type) for rated rotational speed of the propulsion system are shown in Figs.7 to 10.

During computation of the ship vibrations forced by the external non-balanced moments of the main engine, the excitation moments of the order 1., 3., 5. and 8. appear significant for the considered type of the main engine (8S70MC-C). The 1st harmonic component excites mainly vibration of the hull

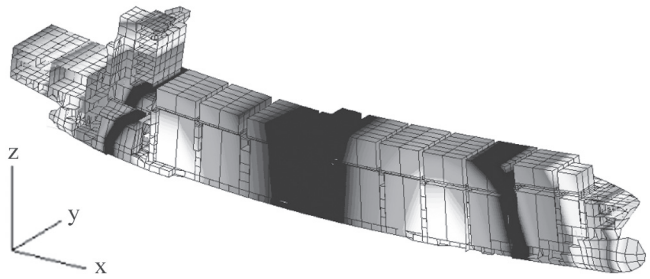

Fig. 7. *Vibrations forced by 1st harmonic component (L and X type) of main engine's external moments*

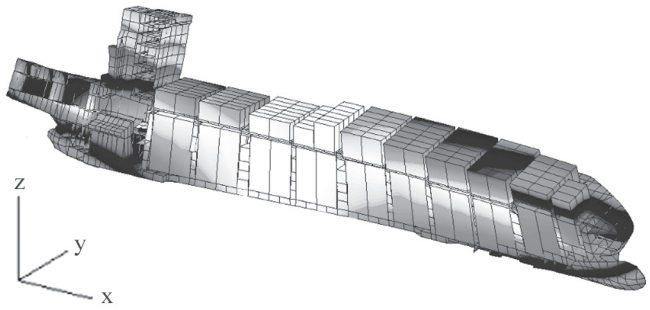

Fig. 8. *Vibrations forced by 3rd harmonic component (X type) of main engine's external moments*

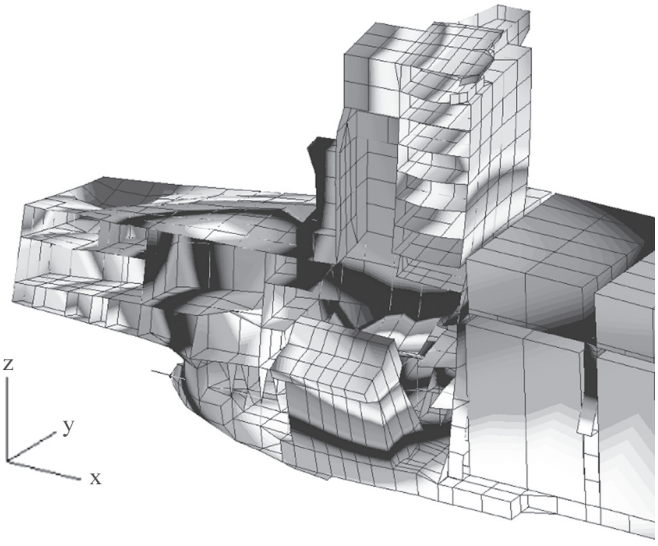

Fig. 9. *Vibrations forced by 5th harmonic component (X type) of main engine's external moments*

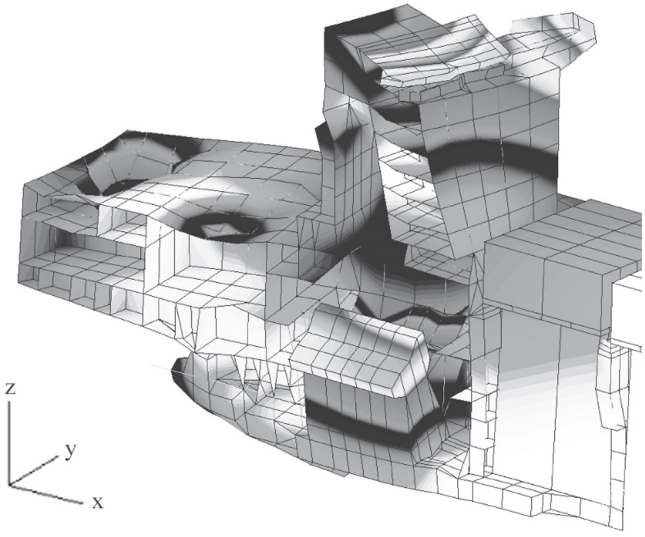

Fig. 10. *Vibrations forced by 8th harmonic component (H type) of main engine's external moments*

structure, whereas the 8th component is responsible for vibration level of the superstructure and main engine (particularly in transverse direction). The excitation forces generated by non-balanced moments of the main engine are responsible particularly for increasing the level of transverse vibrations. For the remaining orientations of vibration other excitation forces are dominating.

OPTIMIZATION OF MUTUAL ANGULAR SETTING OF PROPELLER AND CRANKSHAFT

Two sources of excitations should be taken into account when analyzing the dynamic behaviour of ship hull and superstructure:

- the excitations generated by the propeller and
- those generated by the main engine.

For the propeller-induced excitations the 5th harmonic component is dominating. The engine-induced excitations are represented by full spectrum of harmonic components (8th harmonic component is main for the engine in question), but also the 5th harmonic component is here significant. According to the above presented analyses the levels of expected vibrations forced by the both excitation sources are similar. Phases of the vibrations generated by the propeller depend on a position of the propeller blades, whereas the phases of the vibrations generated by the main engine depend on a position of crankshaft cranks. Therefore mutual phasing of the propeller and crankshaft may considerably affect vibration level of ship superstructure.

Ship superstructure vibrations of each orientation (longitudinal - x, transverse - y, vertical - z) may be optimized (to reduce its level to a minimum). Fig.11 shows the optimum relative angles of angular position of the propeller blade against the first crank of the crankshaft.

Only one angular position of the propeller can be chosen. The highest vibration level is expected for longitudinal orientation of vibration (in x direction). The assumed optimum angle $\alpha = -20.3°$ gives the minimum level of longitudinal vibration at rated rotational speed of the engine.

Fig. 12 presents the total vibration level at the assumed mutual angular phasing of the propeller and crankshaft. It also presents the maximum vibration level (for the worst angular phasing of the propeller : $\alpha = +15.7°$), as well as the minimum one.

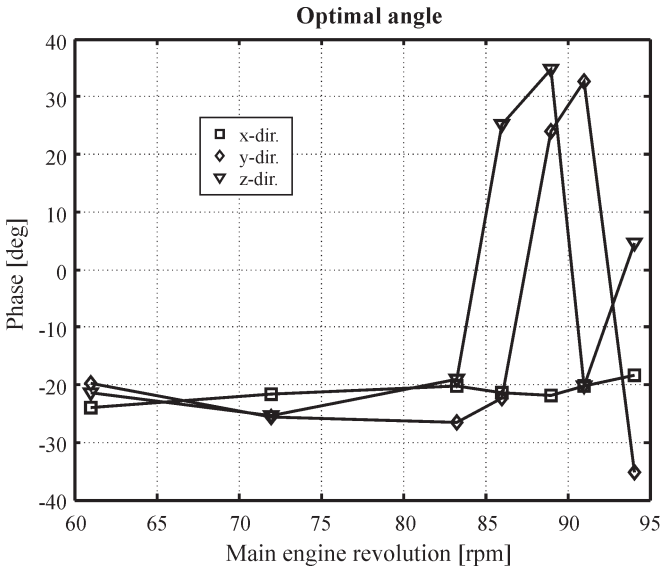

Fig. 11. *Optimum phasing angles of the propeller against the main engine crankshaft*

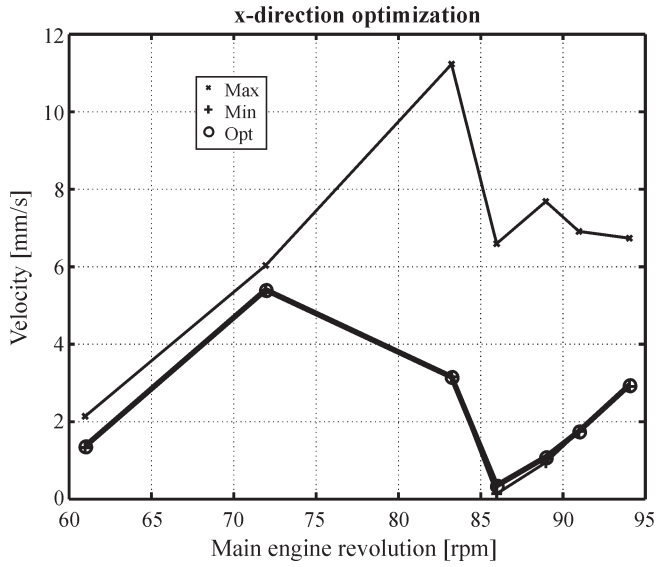

Fig. 12. *Longitudinal vibration velocities of the superstructure (bridge wing) for the optimum phasing of the propeller and main engine crankshaft*

Minimum level of longitudinal vibration may be obtained within a wide range of engine rotational speeds for the optimum angle of propeller angular phasing with respect to the crankshaft. It could be achieved because the optimum angles for this orientation of vibration (x direction) were almost constant in function of engine rotational speed (Fig.11). At the same time the vibration levels for other orientations of vibration (e.g. transverse) may be not optimal, for instance vibration velocity values may be higher than the minimum ones theoretically possible.

The optimum angle value (α = -20.3°) is near to that obtained from another method based on analysis of vibration phases of deckhouse (α = -23.8°). This angle was found by optimizing phases of the forces exciting coupled and non-coupled longitudinal vibrations of the power transmission system. Changes in phases of structural response and other excitation sources were not taken into account. The correctness of the optimum angle was verified by the measurements carried out on the ship in question for different angular positions of the propeller. During sea trial an unacceptable vibration level of the ship superstructure was measured. After changing the relative propeller angle the vibration level measured during next sea trial was reduced as much as three times.

SUMMARY VIBRATIONS – – VERIFICATION BY MEASUREMENTS

The above presented analyzes are based on the hull structural model without added mass of water, for the ship in design load conditions. In order to verify the presented method the forced vibrations should be computed both for the ballast and load conditions by using the mathematical model of the ship with added mass of water. In such mathematical model all the formerly analyzed kinds of excitations were assumed to act simultaneously. Additional independent computations were carried out for the vibrations forced by the main engine and then for those forced by the propeller. The results of these computations can be directly compared with the measurement results [2].

The velocities of the forced vibrations of the ship at rated rotational speed of the propulsion system are shown in Fig.13.

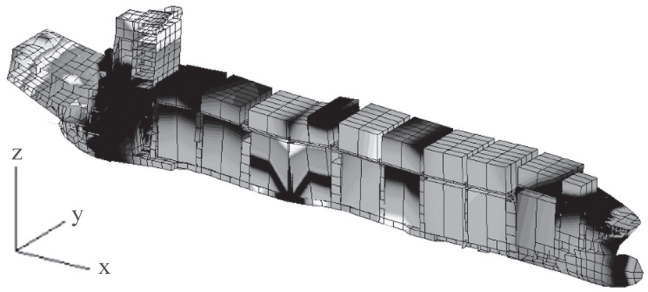

Fig. 13. *Total vibration velocities of the container carrier in design load condition*

Figs.14 and 15 present the diagrams of longitudinal vibration velocities of the superstructure for both considered ship's load conditions, separately for different types of excitation. Possible minimum and maximum vibration levels are also shown. The following notation was used: Prop –excitation by propeller, M.E. – excitation by main engine, Max –maximum vibrations, Min – minimum vibrations, SUM – expected summary vibrations.

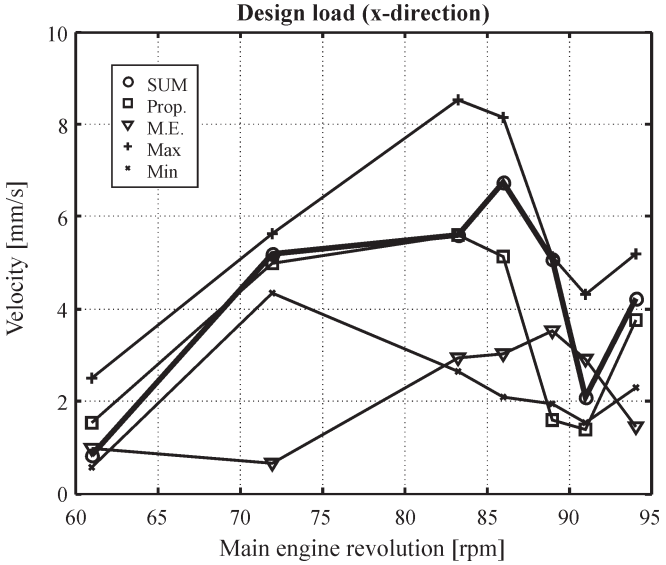

Fig. 14. *Total velocities of longitudinal vibrations of bridge wing (ship in design load conditions)*

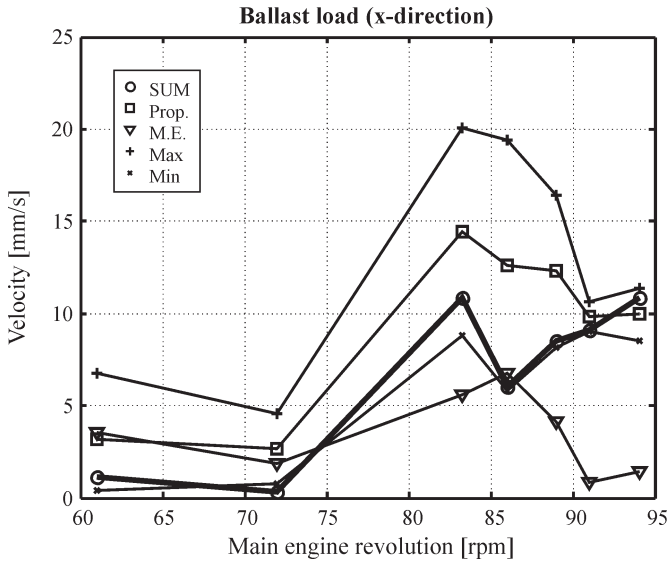

Fig. 15. Total velocities of longitudinal vibrations of bridge wing (ship in ballast conditions)

Figs. 16 and 17 present a comparison of the computation results and ship trial measurement results. The results were converted into rms values of vibration velocity to obtain the customary presentation. The comparison is presented for two essential reference areas : the bridge wing of the superstructure and the transom deck.

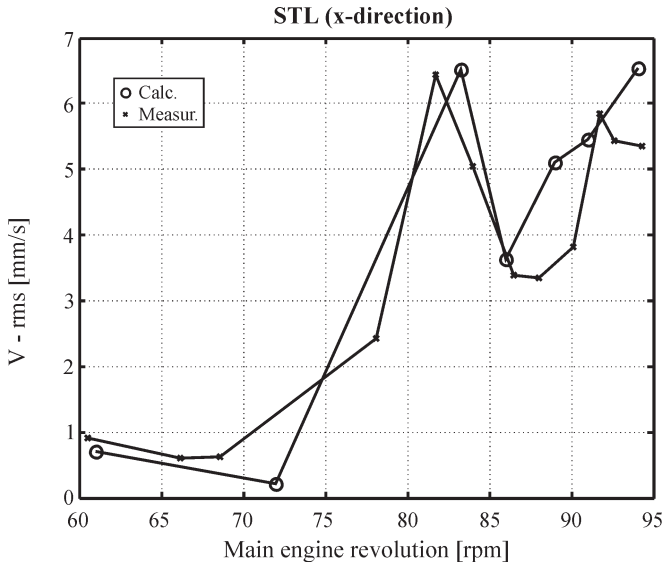

Fig. 16. Verification of the bridge wing vibration: computation results versus measurement results

The forced vibration level is clearly higher for the ship in ballast conditions when compared with that for design load conditions. Sea trials are usually carried out in ballast conditions of the ship and therefore even a correctly designed ship may show excessive vibrations of the superstructure during service. Vertical - horizontal vibrations of the upper part of superstructure are dominating. Comparable vertical vibrations may be also observed for the transom deck.

Magnitude of excitation forces generated by the main engine is similar to that generated by the propeller. Therefore, when analyzing the hull and superstructure vibrations, at least the excitation forces generated by pressure pulses on the transom deck and the forces generated by longitudinal vibration of the power transmission system should be taken into account. Ships of an identical hull structure may show a high or relatively low level of vibration depending on whether its propulsion system is suitably designed. Therefore the complete dynamic analysis of the ship should be carried out simultaneously with its design process – such analysis should be one of its elements.

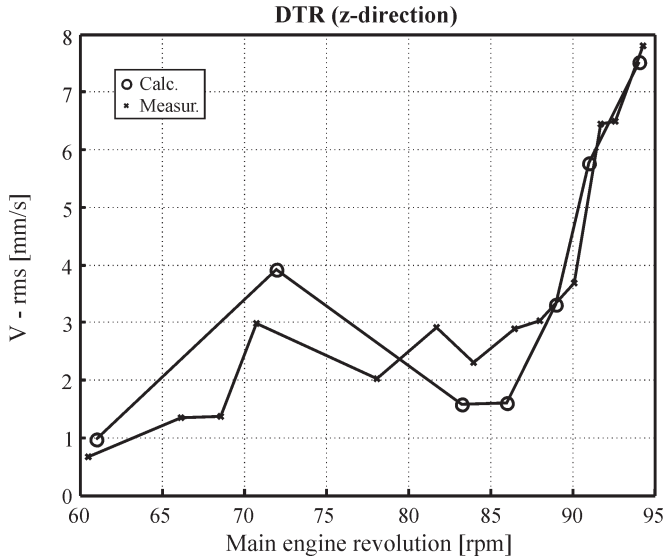

Fig. 17. Verification of the transom deck vibration: computation results versus measurement results

The verification presented in Figs 16 and 17 showing a satisfactory compliance of the numerical computations with measurement results, confirmed that the applied assumptions and computation methods were correct.

RECAPITULATION

- The excitation forces generated by non-balanced moments of the main engine are responsible particularly for increasing the level of transverse vibrations. In the case of dynamic analysis of the container carrier in question other excitation forces are dominating (in longitudinal-vertical direction).
- If levels of the total vibration generated by the propeller and main engine are similar to each other the vibration levels may be optimized by changing the relative angular position of propeller blades and crankshaft. Vibrations of each orientation may be optimized. The longitudinal vibrations expected to be of a high level (excited by main excitation sources: pressure pulses on deck transom and thrust bearing reaction) are usually optimized.
- Forced vibration level is clearly higher for the considered ship in ballast conditions than in design load conditions. The level of excitations generated by the main engine is similar to those generated by the propeller. Therefore, when analyzing the hull and superstructure vibrations, at least the excitation forces generated by pressure pulses on the transom deck and the forces generated by axial vibration of the power transmission system should be taken into account.
- Ships of an identical structure may show a high or relatively low level of vibration depending on whether their propulsion system is suitably designed or not. Therefore a complete dynamic analysis of the ship should be carried out in line with its design process, being one of its elements.
- Correctness of the used assumptions and computation methods was confirmed by the measurements (Figs 16 and 17) as the presented results of the numerical computations and measurements appeared to be in a satisfactory compliance.

ACRONYMS

BRG - bearing
DSLW - coupled vibration of shaftline
DRG - bending vibrations
FEM - Finite Element Method

BIBLIOGRAPHY

1. Chen Yung-Hsiang, Bertran I. M.: *Parametric study of ship - - hull vibrations*. International Shipbuilding Progress, Vol. 37, No 410, July 1990
2. de Bord F., Hennessy W., McDonald J.: *Measurement and analysis of shipboard vibrations.* Marine Technology, Vol. 35, No 1/1998
3. Jakobsen S. B.: *Coupled axial and torsional vibration calculations on long-stroke diesel engine.* The Society of Naval Architects and Marine Engineers, Vol. 99/1991
4. Jenzer J., Welte Y.: *Coupling effect between torsional and axial vibrations in installations with two-stroke diesel engines*. Wartsila NSD. 1991
5. Mumm H: *The need for a more considered design approach to engine-hull interaction.* Proceedings of Lloyds List's Conference on Ship Propulsion Systems. London, 2002
6. Murawski L.: *Influence of journal bearing modelling method on shaft line alignment and whirling vibrations.* PRADS – Eighth International Symposium on Practical Design of Ships and Other Floating Structures. Shanghai-China, Elsevier. 2001
7. Murawski L.: *Axial vibrations of a propulsion system taking into account the couplings and the boundary conditions.* Journal of Marine Science and Technology, Vol. 9, No. 4. Tokyo, 2004
8. Murawski L.: *Shaft line whirling vibrations: effects of numerical assumptions on analysis results*. Marine Technology and SNAME (Society of Naval Architects and Marine Engineering) News, Vol. 42, April 2005
9. Rao T., Iyer N., Rajasankar J., Palani G.: *Dynamic response analysis of ship hull structures.* Marine Technology, Vol. 37, No. 3/2000
10. Thorbeck H., Langecker E.: *Evaluation of damping properties of ship structures*. Schiffbauforschung, No. 39/2000
11. MAN B&W Diesel A/S : *Shafting alignment for direct coupled low-speed diesel propulsion plants*. Copenhagen, 1995
12. Germanischer Lloyd : *Ship vibration.*, Issue No. 5/2001

CONTACT WITH THE AUTHOR

Lech Murawski, D.Sc.,M.E.
Ship Design and Research Centre
Rzeczypospolitej 8
80-369 Gdańsk, POLAND
e-mail : Lech.Murawski@cto.gda.pl

Conference

Diagnostics of machines

Faculty of Transport,
Silesian University of Technology, organized

32nd Domestic Symposium on Diagnostics of Machines

which took place on 28 February ÷ 05 March, 2005 at Węgierska Górka, a south-Poland mountain resort.

It was held within the frame of 60th anniversary of Silesian University of Technology and 35 years of activity of „Transport" education line.

Scientific program of the already traditional meeting of experts in diagnostics contained broad spectrum of topics covered by 60 papers prepared by representatives of 16 Polish universities and scientific research centres.

The greatest number of papers was presented by scientific workers from Silesian University of Technology (15) and Warsaw University of Technology (11). Maritime specialists offerred 12 papers :

- *Use of current signals for diagnosing bow thrusters* by T. Burnos (Technical University of Szczecin)
- *Diagnosing ship propulsion systems on the basis of measurement of operational parameters* – by A. Charchalis (Gdynia Maritime University)
- *Service investigations of starting and rundown processes of LM 2500 ship gas turbine* – by A.Charchalis (Gdynia Maritime University) and P. Wirkowski (Polish Naval University)
- *Making operational decisions with taking into account likelihood of diagnosis on technical state of machine* by J. Girtler (Gdańsk University of Technology)
- *Analysis of trends of vibration parameters of ship gas turbines* – by A. Grządziela (Polish Naval University)
- *Assessment of state of injectors of driving engine of synchronous electric generator on the basis of its electric energy parameters* – by G. Grzeczka (Polish Naval University)
- *Endoscopic diagnostics of ship engines* – by Z. Korczewski and B. Pojawa (Polish Naval University)
- *Subject-matter analysis of trend of changes of metallic impurities in lubricating oil of ship gas turbines* by M. Mironiuk (Polish Naval University)
- *Expertise of cause of a failure of piston-rod stuffing--box of a ship low-speed diesel engine* – by L. Murawski (Ship Design & Research Centre, Gdańsk)
- *Diagnostics of underwater objects by using ROV vehicles* – by A. Olejnik (Polish Naval University)
- *Technical state assessment of injection devices of self--ignition engine on the basis of indication diagram's course* – by R. Pawletko (Gdynia Maritime University)
- *Ship double-rotor gas turbine as an object of modelling* – by P. Wirkowski (Polish Naval University).

Numerical simulation of heat flow processes

Andrzej Mielewczyk
Gdynia Maritime University

ABSTRACT

Numerical simulation method is based on mathematical models of physical processes, which describe run of a given process with a various accuracy. This paper presents a method for elaborating the computer simulation models based on differential equations. This makes it possible to obtain a high accuracy of representing dynamic features of a real process. The derived results are given in the form of numerical series. An example of modelling the dynamics of heat transfer through a flat wall is presented in the second part of the paper. Basing on the model one can simulate the process of operation of ship engine as well as such auxiliary devices as a cooler, evaporator, condenser, tank heating system etc.

Keywords : simulation, dynamic model, heat transfer, **Z** - transform

INTRODUCTION

Computer simulation has presently become a common tool. Simulators are used in didactic process, scientific research, and training courses, especially for operators. This way they substitute real technical devices, for economical and safety reasons. Today operational and maintenance conditions of machines are closer and closer to those represented in simulators. Educational process of to-be operators of machines starts from using the simulators.

The simulation makes it possible to represent difficult and dangerous operational situations and to learn to give an appropriate response to hazards. A boundary between a real situation and simulated one becomes obliterated. A simulation must be close to reality in order an operator always could consider a given situation as real one. By continuous improving the simulators a higher and higher level of education and safety can be ensured.

Developments in process automation and control have made it necessary to have at one's disposal a model of a given process [8, 9, 12].

By comparing a model of a given process with its real run it is possible to determine an instantaneous point of operation select appropriate control parameters and generate a correct message for operator, that rises safety level of the process. Simulation has also found wide application in training of sea-going ship's operators, both navigators and marine engineers. Hence simulators have become an indispensable instrumentation of maritime academies.

Simulation approach has also its important place in forming new scientific theories and widening the knowledge. In this way one looks for confirmation of laws in engineering, physics, economy and medicine. An expected chance for space missions is also checked by means of simulations.

In this paper has been presented the problem of modelling heat flow processes by using **Z -** transform applied to differential equation of a modeled process. This facilitates elaborating the digital models on which the work of any simulator is based.

SIMULATION MODELLING

During process simulation one tends to exactly represent statical and dynamical features of a given process. A simulation model should appropriately respond to external signals, and in the case of some kinds of simulators it should provide real-time responses. Real processes are complex and depending on many parameters. Only the simulation models based on differential equations are capable in providing a high conformance with real processes [10,14]. To find solutions of such equations is time-consuming. Modelling the objects of complex parameters leads to partial differential equations [1, 3, 4, 11]. For this reason one often introduces simplifications in expense of accuracy of process representation. For example, either simple algebraic equations are introduced, or process statical and dynamical features are separately considered . However the so seperated dynamical term does not account for all variables of the object in question.

Applying another approach one substitutes finite difference equations for differential equations, that impairs accuracy of solution. In solving partial differential equations by means of

the finite difference method a condition for stability of solution is introduced [13]. For instance the heat transfer equation :

$$\frac{\partial U(x,t)}{\partial t} = a\frac{\partial^2 U(x,t)}{\partial x^2} \tag{1}$$

obtains, after digitization respective to time and spatial variable, the following form of response in successive time instants :

$$U(x_i,t_{n+1}) = a\frac{T}{\Delta x^2}U(x_{i-1},t_n) + \left(1-2a\frac{T}{\Delta x^2}\right)U(x_i,t_n) + a\frac{T}{\Delta x^2}U(x_{i+1},t_n) \tag{2}$$

To reach a higher calculation accuracy a digitizing step, both in the time and space domain, is made shorter and simultaneously the following stability condition has to be satisfied :

$$a\frac{T}{\Delta x^2} \le \frac{1}{2} \tag{3}$$

The time step T is imposed by the assumed digitizing step Δx. The application of a variable digitizing step is necessary to accelerate a response being always of recurrent type. How to find a compromise between simulation accuracy and its duration time is an open question. During simulation process much time is usually devoted to graphical presentation of a model.

This author has proposed to combine the advantages of solving differential equations and finite difference ones in order to determine process models.

The digitization is applied respective to the time variable **t** only. Equations in such a form can be solved with the use of the transform **Z**. The time variable **t** passes into **z** and becomes a parameter. The so obtained equation can be solved respective to spatial variables as continuous one by integrating it and applying the known methods for solving partial differential equations, e.g. the method of separation of variables or that of successive integral transformations [5]. In this phase dynamic relations of modeled process is not solved. Now the inverse transformation **Z** of the initial function is made to obtain its course respective to time.

The proposed approach makes it possible to obtain a solution equivalent to continuous one. This way the digitization in the domain of spatial variables as well as the necessity to satisfy the associated stability condition, is avoided. The digitization in the time domain only enables to choose indpendently a time step limited only by an assumed solution accuracy. The inverse transform **Z** is calculated by expanding the function into numerical series by means of the following formula [6]:

$$f_n = \lim_{p\to 0}\frac{1}{n!}\frac{d^n F\left(z=\frac{1}{p}\right)}{dp^n} \tag{4}$$

If an expansion of a given function into Taylor series respective to the variable *p* exists then it is always possible to determine a solution. This is much easier to do than to use the Laplace transform [2, 7, 10]. The final solution contains all process variables and the time variable in a discrete form. The result is yielded in the form of numerical series, which leads to simple procedures of numerical programming; the calculation error depends on digitizing the function respective to time, only.

In each computational step the process parameters take constant values. In Eq.(1) the parameter **a** is constant and not dependent on time and position. The parameters can be changed in successive computational steps. The equation is reduced to a differential equation of constant coefficients, and a linear form of a given model is obtained.

EXAMPLE: HEAT TRANSFER THROUGH A WALL

Heat transfer through a flat wall occurs in many ship systems and technical devices. The phenomenon is described by Eq.(1) which can be solved by using the proposed method. After application of the transform **Z** the Eq. (1) takes the following form :

$$\frac{d^2U(x,z)}{dx^2} - \frac{1}{aT}\frac{z-1}{z}U(x,z) = 0 \tag{5}$$

where :

$$a = \frac{\lambda}{\rho c}$$

After transformation one can obtain a parabolic 2nd order differential equation of constant coefficients. Its solution is as follows :

$$U(x,z) = Ae^{r_1 x} + Be^{r_2 x} \tag{6}$$

where :

$$r_{1,2} = \mp\frac{1}{\sqrt{aT}}\sqrt{\frac{z-1}{z}} \tag{7}$$

In order to solve Eq.(5) the following boundary conditions have been defined :

1. Temperature on the inner side of the wall varies in compliance with the assumed function :

$$U(0,z) = A + B = U_0(z) \tag{8}$$

2. The outer side of the wall is insulated, hence :

$$-\lambda\frac{dU(x=w,z)}{dx} = -\lambda\left(Ar_1e^{r_1 x} + Br_2e^{r_2 x}\right) = 0 \tag{9}$$

The solution of Eq.(5) is described by the following formula :

$$U(x,z) = U_0(z)\frac{e^{r_1(x-w)} + e^{r_2(x-w)}}{e^{r_1 w} + e^{r_2 w}} \tag{10}$$

The wall's outer side temperature is described by the formula :

$$U(w,z) = U_0(z)\frac{2}{e^{\frac{w}{\sqrt{aT}}\sqrt{\frac{z-1}{z}}} + e^{-\frac{w}{\sqrt{aT}}\sqrt{\frac{z-1}{z}}}} \tag{11}$$

Finally, it is necessary to calculate the inverse transform **Z** by using the relation (4) :

$$F(z) = e^{\alpha\sqrt{\frac{z-1}{z}}} + e^{-\alpha\sqrt{\frac{z-1}{z}}} \tag{12}$$

where :

$$\alpha = \frac{w}{\sqrt{aT}}$$

The inverse transform is obtained this way :

$$f(nT) = 0,-1,-\sum_{n=2}^{\infty}\frac{1}{2^{2n-3}}\frac{(2n-3)!}{n!(n-2)!}\alpha\sinh\alpha-\sum_{n=3}^{\infty}\sum_{k=1}^{\frac{n-1}{2},\frac{n-2}{2}}\frac{1}{2^{2n-2k-2}}\frac{(n-k-1)(2n-2k-3)!}{kn!(2k-1)!(n-2k-1)!}\alpha^{2k+1}\sinh\alpha+$$
$$+2\cosh\alpha,0,\sum_{n=2}^{\infty}\sum_{k=0}^{\frac{n-3}{2},\frac{n-2}{2}}\frac{1}{2^{2n-2k-3}}\frac{(2n-2k-3)!}{n!(2k+1)!(n-2k-2)!}\alpha^{2k+2}\cosh\alpha \tag{13}$$

A choice of **k** value is realized in accordance with the following principle :

k = 1 for odd values of n ; k = 2 for even values of n

The exciting function $\mathbf{U}_0(z)$ may be arbitrary, however this leads to the operation of convolution. If $\mathbf{U}_0(z)$ is assumed a step function then the response is a sum of terms of given series. This way the mentioned operation of convolution can be avoided. For realization of other functions the approximation by a staircase function is advised. Such approximation method is used for digital control algorithms.

In the time domain Eq.(11) takes the form :

$$U(w,nT) = U_0\frac{2}{a_0+a_1+a_2+a_3+\ldots+a_{n-1}+a_n} \tag{14}$$

where :

$$a_0 = 2\cosh\alpha\ ;\ a_1 = -\alpha\sinh\alpha\ ;\ a_2 = -\frac{1}{4}\alpha\sinh\alpha+\frac{1}{4}\alpha^2\cosh\alpha\ ;\ a_3 = -\frac{3}{24}\alpha\sinh\alpha+\frac{3}{24}\alpha^2\cosh\alpha-\frac{1}{24}\alpha^3\sinh\alpha$$

. . . . . .

$$a_n = -\frac{1}{2^{2n-3}}\frac{(2n-3)!}{n!(n-2)!}\alpha\sinh\alpha-\sum_{k=1}^{\frac{n-1}{2},\frac{n-2}{2}}\frac{1}{2^{2n-2k-2}}\frac{(n-k-1)(2n-2k-3)!}{kn!(2k-1)!(n-2k-1)!}\alpha^{2k+1}\sinh\alpha+$$
$$+\sum_{k=0}^{\frac{n-3}{2},\frac{n-2}{2}}\frac{1}{2^{2n-2k-3}}\frac{(2n-2k-3)!}{n!(2k+1)!(n-2k-2)!}\alpha^{2k+2}\cosh\alpha \tag{15}$$

After dividing by the series $\mathbf{a}_n$ the response at discrete instants is obtained. For the exciting step signal it amounts to :

$$U(w,nT) = U_0\frac{1}{\cosh\alpha}\left(\begin{array}{l}\dfrac{1}{2^{2n-2}}\dfrac{(2n-3)!}{n!(n-2)!}\alpha\tanh\alpha+\\ +\displaystyle\sum_{k=1}^{\frac{n-1}{2},\frac{n-2}{2}}\sum_{m=0}^{k}\frac{1}{2^{2n-2k-1}}\frac{(n-k-1)(2n-2k-3)!}{kn!(2k-1)!(n-2k-1)!}\alpha^{2k+1}D_{2k+1,m}\tanh^{2m+1}\alpha+\\ +\displaystyle\sum_{k=0}^{\frac{n-3}{2},\frac{n-2}{2}}\sum_{m=0}^{k}\frac{1}{2^{2n-2k-2}}\frac{(2n-2k-3)!}{n!(2k+1)!(n-2k-2)!}\alpha^{2k+2}D_{2k,m}\tanh^{2m}\alpha\end{array}\right) \tag{16}$$

The coefficients $D_{k,m}$ are derived from the recurrence algorithm based on the Pascal triangle principle, namely from the formulae (17 and 18) :

$$\begin{array}{lccccccc}
k=1 & & & 1 & & & & \\
k=2 & & & 1 & & -2! & & \\
k=3 & & & 1 & & -3! & & \\
k=4 & & 1 & & -10\cdot 2! & & 4! & \\
k=5 & & 1 & & -10\cdot 3! & & 5! & \\
k=6 & 1 & & -91\cdot 2! & & 35\cdot 4! & & -6! \\
k=7 & 1 & & -91\cdot 3! & & 35\cdot 5! & & -7! \\
k=8 & 1 & -820\cdot 2! & & 966\cdot 4! & & -84\cdot 6! & 8! \\
k=9 & 1 & -820\cdot 3! & & 966\cdot 5! & & -84\cdot 7! & 9! \\
k=10 & 1 & -7381\cdot 2! & 24970\cdot 4! & & -5082\cdot 6! & 165\cdot 8! & -10! \\
k=11 & 1 & -7381\cdot 3! & 24970\cdot 5! & & -5082\cdot 7! & 165\cdot 9! & -11!
\end{array}$$

. . . . . .

$$\begin{cases} D(2k+1,m) = (-1)^m \left[D_1(2k-1,m) + (2m+1)^2 D_1(2k-1,m) \right] (2m+1)! \\ D(2k,m) = (-1)^m \left[D_1(2k-2,m) + (2m+1)^2 D_1(2k-2,m) \right] (2m)! \end{cases} \quad (17)$$

$$D_{k,m} = \sum_{i=m}^{k} (-1)^m \frac{i!}{k!(i-k)!} D(k,i) \quad (18)$$

For m=0 the Euler numbers are yielded [15] :

$$D_{k,0} = \sum_{i=0}^{k} D(k,i) = E_k \quad (19)$$

The successive values of the function are as follows :

$$U(w,0) = 0$$

$$U(w,T) = U_0 \frac{1}{\cosh \alpha}$$

$$U(w,2T) = U_0 \frac{1}{\cosh \alpha} \left(1 + \frac{1}{2} \alpha \tanh \alpha \right)$$

$$U(w,3T) = U_0 \frac{1}{\cosh \alpha} \left(1 + \frac{1}{2} \alpha \tanh \alpha + \frac{1}{8} \alpha \tanh \alpha + \left[-\frac{1}{8} + \frac{1}{4} \tanh^2 \alpha \right] \alpha^2 \right)$$

Below in the figure results of the example calculations performed by using the described method are presented.

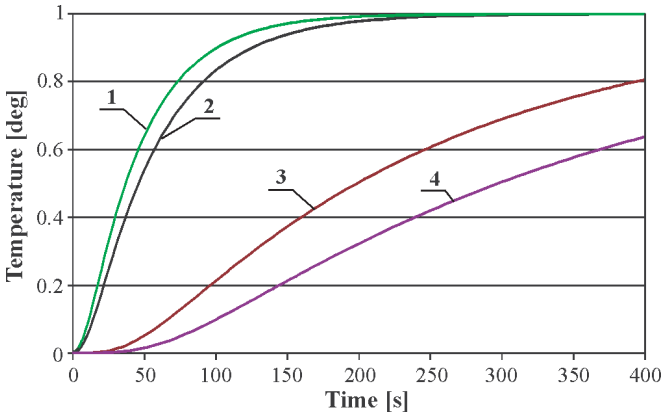

Dynamic characteristics of heat transfer through the wall of 0.1 m in thickness, the excitation $U_0(t)$ = 1[deg], for the following materials : 1 – copper; 2 – aluminium; 3 – brass; 4 – steel.

RECAPITULATION

The presented method has many advantages, namely :

- Simulation time is very short since any particular term of the series represents a solution.
- Calculations can be extended by means of non-zero initial conditions and arbitrary boundary conditions. This does not impair accuracy of the model.
- A simulation step may be chosen from a wide variability range. It makes calculation time shortening possible that is demanded during simulation to disregard its already known fragments.
- In some selected cases the model in question enables to determine a response value at n-th instant with disregarding the preceding ones. The so obtained solution is equivalent to continuous one.

NOMENCLATURE

a – coefficient of temperature equalization [m²/s]
a_n – coefficients of numerical series
A, B – integration constants
c – specific heat of a material [J/kgK]
D – coefficients of expanded form of a initial function
n – natural number
r_1, r_2 – zero loci of a partial differential equation
t – time[s]
T – digitizing period [s]
U – temperature function
U_o – initial values
w – wall thickness [m]
x – spatial variable
z, p – arguments of a function in the complex variable domain
λ – thermal conductance [W/mK]
ρ – density [kg/m³]

BIBLIOGRAPHY

1. Douglas J. M.: *Dynamics and control of processes . Analysis of dynamic systems* (in Polish). WNT (Scientific - Technical Publishing House). Warszawa, 1976
2. Friedly J. C.: *Analysis of dynamics of processes* (in Polish). WNT. Warszawa, 1975
3. Gdula S. J. (Editor). : *Heat transfer* (in Polish). PWN (State Scientific Publishing House). Warszawa, 1984
4. Hobler T.: *Thermal motion and heat exchangers* (in Polish). WNT. Warszawa, 1979
5. Kącki E.: *Partial differential equations in physics and engineering* (in Polish). WNT. Warszawa, 1992
6. Kudrewicz J.: *Z- transform and finite difference equations* (in Polish). PWN, Warszawa, 2000
7. Mielewczyk A.: *A simulation model of control process for cooling and lubricating systems of a medium-speed combustion engine* (in Polish). Doctorate thesis. Gdańsk University of Technology, Faculty of Ocean Engineering and Ship Technology. Gdańsk, 1998
8. Mielewczyk A.: *Computer simulation of control processes of ship power plant auxiliary systems.* Polish Maritime Research, Vol.7, No.3(25) September 2000
9. Mielewczyk A.: *A simulation model of plate cooler.* Polish Maritime Research, Vol.8, No 3(29) September 2001
10. Mikielewicz J.: *Modeling of heat flow processes* (in Polish). Institute of Fluid Flow Machinery, Polish Academy of Sciences. Wrocław, 1995
11. Petela R.: *Heat flow* (in Polish). PWN. Warszawa, 1983
12. Piekarski M., Poniewski M.: *Dynamics and control of processes of heat and mass exchange* (in Polish). WNT. Warszawa, 1994
13. Taler J., Duda P.: *Solving the simple and inverse heat flow problems* (in Polish). WNT. Warszawa, 2003
14. Tarnowski W.: *Modelling of systems* (in Polish). (Publishing House of Koszalin University of Technology) Wydawnictwo Uczelniane Politechniki Koszalińskiej. Koszalin, 2004
15. Weisstein W. E.: *Interactive mathematics encyclopedia*. Wolfram Research Inc, www.mathworld.wolfram.com

CONTACT WITH THE AUTHOR

Andrzej Mielewczyk
Department of Basic Engineering Sciences,
Gdynia Maritime University
Morska 81-87
81-225 Gdynia, POLAND
e-mail : mieczyk@am.gdynia.pl

An algorithm for determining permissible control inputs to unmanned Underwater Robotic Vehicle (URV) fitted with azimuth propellers

Jerzy Garus
Polish Naval University

ABSTRACT

The paper deals with synthesis of automatic control system for an unmanned underwater robotic vehicle. The problem of determining permissible propulsive forces and moments necessary for optimum power distribution within a propulsion system composed of azimuth propellers (rotative ones). To allocate thrusts the unconstrained optimization method making it possible to obtain a minimum-norm solution, was applied. A method was presented for assessing propulsion system capability to generate propulsive forces (set control inputs). For the case of lack of such capability an algorithm was proposed making modification of their values and determination of feasible propulsive forces (i.e. permissible control inputs), possible. A numerical example which confirmed correctness and effectiveness of the proposed approach, was also attached.

Keywords : underwater vehicle, propulsion system, azimuth propeller, control

INTRODUCTION

Underwater Robotic Vehicles (URV) play an important role among various technical means used for searching seas and oceans. The unmanned floating units fitted with propulsors and capable of maneouvring are designed to realize tasks at the water depth from a dozen or so to several thousand meters.

Robot's motion of six degrees of freedom is described by means of the following vectors [1, 3] :

$$\boldsymbol{\eta} = [x,\ y,\ z,\ \phi,\ \theta,\ \psi]^T$$
$$\mathbf{v} = [u,\ v,\ w,\ p,\ q,\ r]^T \qquad (1)$$
$$\boldsymbol{\tau} = [X,\ Y,\ Z,\ K,\ M,\ N]^T$$

where :

- $\boldsymbol{\eta}$ – vector of location and orientation in an inertial reference system
- $\mathbf{v}$ – vector of linear and angular velocities in a hull-fixed reference system
- $\boldsymbol{\tau}$ – vector of forces and moments acting on the robot in a hull-fixed reference system.

Contemporary underwater robots are often and often equipped with the automatic control systems which make it possible to execute complex maneuvers and operations without any intervention of operator. The main modules of such control system are shown in Fig.1. Its crucial element is the autopilot which – on the basis of comparison of a current location of controlled object with its set values – determines forces and moments to be generated by the propulsion system so as to make the object's behavior complying with that assumed. The thrust vector corresponding with them is computed in the thrust distribution module and sent to the propulsion system as a control quantity.

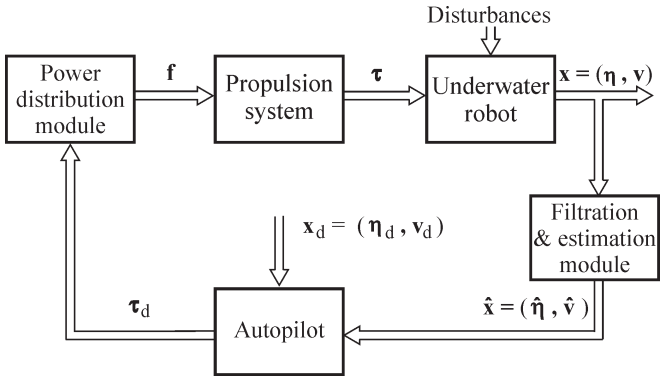

Fig. 1. *Schematic diagram of a control system for underwater robot*

The control laws implemented in the autopilot , which make it possible to determine propulsive forces and moments, have a general character; they do not take into account constraints put on maximum and minimum values of the thrusts which can be developed by particular propellers. It can cause that the obtained solution would be unfeasible for the propulsion system. Such situation may worsen control quality and cause that robot's behavior would greatly differ from that assumed.

Therefore a two-phase procedure
of power distribution is proposed (Fig.2).

In the first phase propulsion system capability of generating the set control inputs $\boldsymbol{\tau}_d$ would be assessed and the permissible control inputs $\boldsymbol{\tau}'_d$ (i.e. such values of forces and moments which the propulsion system is able to generate) would be determined. Their values would be so calculated as – ensuring operation of propellers to a saturation limit at most – not to cause a drastic perturbation in the robot's motion control process.

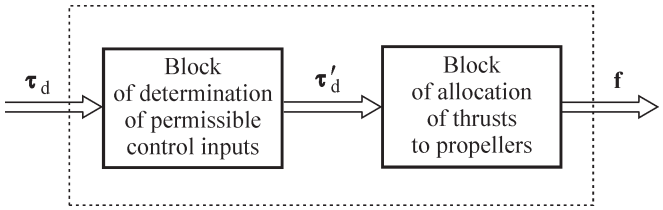

Fig. 2. Schematic diagram of power distribution module

In the second phase on the basis of $\boldsymbol{\tau}'_d$ the thrust vector **f** would be calculated, i.e. the allocation of thrusts to particular propellers would be performed.

THRUST ALLOCATION PROCEDURE FOR HORIZONTAL MOTION

The solution used in majority of conventional unmanned underwater robots is a structure having longitudinal and transverse metacentric stability which ensures motion with small trim and heel angles. Hence the basic motion of such objects is their translation in horizontal plane at changing depth of immersion, being a motion of four degrees of freedom.

It makes it possible to split the propulsion system
into two independent subsystems, namely :

- vertical motion subsystem (in vertical plane)
- horizontal motion subsystem (in horizontal plane).

The first produces the propulsive force acting along vertical axis, and the second ensures translational motion along longitudinal and transverse axes and rotation around vertical axis.

In this paper an underwater robot is considered fitted with the propulsion system having the arrangement of propellers shown in Fig.3. Its vertical motion subsystem consists of two vertically arranged, ducted screw propellers. To assess capability of the subsystem to generate the set force Z_d is not a difficult task as its absolute value cannot exceed the sum of maximum thrusts developed by the propellers [4].

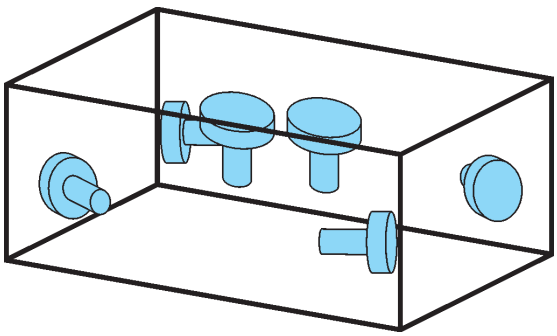

Fig. 3. Arrangement of the propulsion system fitted with six propellers

The horizontal motion subsystem consists of four spatially arranged azimuth propellers producing forces along longitudinal and transverse axes as well as moment of force in vertical axis. To assess capability of the subsystem to generate the set forces X_d and Y_d as well as the moment N_d is a complex task as each of the propellers contributes to generating both propulsive forces and propulsive moment. Therefore it is necessary to have a procedure making it possible to assess whether the set control inputs are feasible, and in the case if the subsystem is not capable to produce them to modify them in such a way as to ensure their feasible values. Hence further considerations are limited to plane horizontal motion of the robot.

Let $\boldsymbol{\tau}_d = [\tau_{d1}, \tau_{d2}, \tau_{d3}]^T = [X_d, Y_d, N_d]^T$ stand for the vector of set propulsive forces and propulsive moment, and $\mathbf{f} = [f_1, f_2, f_3, f_4]^T$ - for the vector of thrusts developed by the propellers.

Moreover let the components of the vectors
be constrained by the following constraints :

$$\tau_{dj}^2 - \left(\tau_j^{max}\right)^2 \le 0 \qquad \text{for} \quad j = \overline{1,3} \tag{2}$$

$$f_i^2 - \left(f_i^{max}\right)^2 \le 0 \qquad \text{for} \quad i = \overline{1,4} \tag{3}$$

resulting from design parameters, arrangement and orientation of the propellers within the hull of the robot.

The vector of forces and moment, $\boldsymbol{\tau}$, is associated with the thrust vector **f** by means of the following relationship [1,2] :

$$\boldsymbol{\tau}_d = \mathbf{T}(\boldsymbol{\alpha})\mathbf{f} \tag{4}$$

where :

$\mathbf{T}(\boldsymbol{\alpha})$ – arrangement matrix of propellers :

$$\mathbf{T}(\boldsymbol{\alpha}) = \tag{5}$$

$$= \begin{bmatrix} \cos(\alpha_1) & \cos(\alpha_2) & \dots & \cos(\alpha_4) \\ \sin(\alpha_1) & \sin(\alpha_2) & \dots & \sin(\alpha_4) \\ d_1 \sin(\alpha_1 - \varphi_1) & d_2 \sin(\alpha_2 - \varphi_2) & \dots & d_4 \sin(\alpha_4 - \varphi_4) \end{bmatrix}$$

$\boldsymbol{\alpha} = [\alpha_1, \alpha_2, \dots, \alpha_4]^T$ – vector of thrust angles
α_i – thrust angle of i-th propeller, i.e. the angle between vehicle's longitudinal axis and direction of its thrust force
φ_i – orientation angle of i-th propeller, i.e. the angle between vehicle's longitudinal axis and the line connecting the vehicle's mass centre and the propeller axis
d_i – distance of i-th propeller from the vehicle's mass centre.

The quantities α_i, φ_i and d_i are shown in Fig.4.

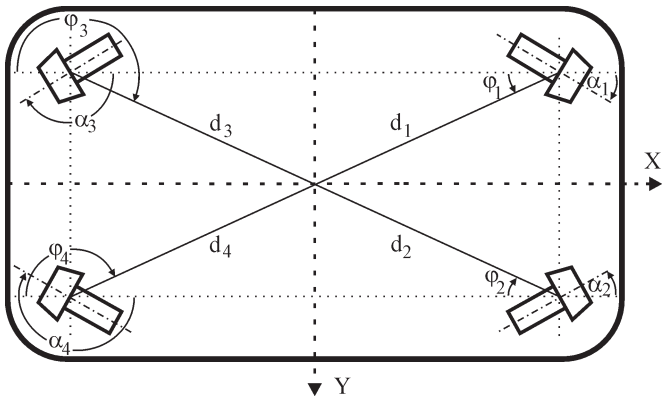

Fig. 4. Arrangement of 4 propellers in horizontal motion subsystem

The propellers are aimed at developing such thrusts which can ensure generating the vector of set control inputs $\boldsymbol{\tau}_d = [\tau_{d1}, \tau_{d2}, \tau_{d3}]^T$. Allocation of thrust values to particular propellers is realized in the power distribution module. The problem of

determination of values the thrust vector **f** on the basis of the vector of set control inputs $\boldsymbol{\tau}_d$ is usually considered as an unconstrained optimization problem in which a minimum-norm solution is searched for. The solution has the following form [1,5] :

$$\mathbf{f} = \mathbf{T}^*(\boldsymbol{\alpha})\boldsymbol{\tau}_d \tag{6}$$

where :

Moore-Penrose's pseudo-inverse matrix :

$$\mathbf{T}^*(\boldsymbol{\alpha}) = \mathbf{T}^T(\boldsymbol{\alpha})[\mathbf{T}(\boldsymbol{\alpha}) \cdot \mathbf{T}^T(\boldsymbol{\alpha})]^{-1}$$

Its practical application is possible then and only then, when no demand of developing a thrust value exceeding the limit value (3) by anyone of the thrust propellers is declared. If it is the case then the set control inputs cannot be generated and a modification of their values is necessary, i.e. determination of the vector of permissible control inputs $\boldsymbol{\tau}'_d = [\tau'_{d1}, \tau'_{d2}, \tau'_{d3}]^T$. Together with the vector of control inputs the vector of azimuth angles is computed. A way of determining their values is presented below.

ALGORITHM FOR DETERMINING THE VECTOR OF PERMISSIBLE CONTROL INPUTS

Let the robot's propulsion subsystem ensuring its planar horizontal motion be consisted of four azimuth propellers of the following features :

- of the same type, hence the thrust $f_i^{max} = f_k^{max} = f^{max}$ for $i,k = \overline{1,4}$
- located at the same distance from the mass centre, symmetrically against the robot's plane of symmetry, namely :

  $d_i = d_k = d$ and $\varphi_i \bmod \frac{\pi}{2} = \varphi_k \bmod \frac{\pi}{2} = \varphi$ for $i,k = \overline{1,4}$
- whose thrust angles satisfy the relationships :
  - at every instant t for $i,k = \overline{1,4}$ and $i \neq k$:

$$\begin{aligned}
&\alpha_i(t) \bmod \frac{\pi}{2} = \alpha_k(t) \bmod \frac{\pi}{2} = \alpha(t)\\
&0 < \alpha_{min} \le \alpha(t) \le \alpha_{max} = \frac{\pi}{2} - \alpha_{min}\\
&\left|\sin[\alpha_i(t)]\right| = \left|\sin[\alpha_k(t)]\right| = \sin[\alpha(t)]\\
&\left|\cos[\alpha_i(t)]\right| = \left|\cos[\alpha_k(t)]\right| = \cos[\alpha(t)]\\
&\left|\sin[\alpha_i(t) - \varphi_i]\right| = \left|\sin[\alpha_k(t) - \varphi_k]\right| = \sin[\alpha(t) + \varphi]
\end{aligned} \tag{7}$$

  - thrust angle change by the value $\pm\Delta\alpha$ occurs in all the propellers simultaneously.

By virtue of the above given assumptions and the relationship (4) the forces and moment at the instant t are described by the following equations :

$$\begin{aligned}
\tau_1[\alpha(t)] &= \sum_{i=1}^{4} \cos[\alpha_i(t)] f_i =\\
&= \cos[\alpha(t)] \sum_{i=1}^{4} \operatorname{sign}\{\cos[\alpha_i(t)]\} f_i
\end{aligned} \tag{8}$$

$$\begin{aligned}
\tau_2[\alpha(t)] &= \sum_{i=1}^{4} \sin[\alpha_i(t)] f_i =\\
&= \sin[\alpha(t)] \sum_{i=1}^{4} \operatorname{sign}\{\sin[\alpha_i(t)]\} f_i
\end{aligned} \tag{9}$$

$$\begin{aligned}
\tau_3[\alpha(t)] &= \sum_{i=1}^{4} d_i \sin[\alpha_i(t) - \varphi_i] f_i =\\
&= d \sin[\alpha(t) + \varphi] \sum_{i=1}^{4} \operatorname{sign}\{\sin[\alpha_i(t) - \varphi_i]\} f_i
\end{aligned} \tag{10}$$

where :

$\tau_1[\alpha(t)]$, $\tau_2[\alpha(t)]$- propulsive forces along longitudinal and transverse axis, respectively

$\tau_3[\alpha(t)]$- force moment around vertical axis.

(To make the mathematical description more clear, the time symbol t in the notation of the thrust angle $\alpha(t)$ is further omitted).

The maximum values of the quantities, possible to be generated by the propulsion system are as follows :

$$\begin{aligned}
\tau_{1max} &= \max_{\alpha_{min} \le \alpha \le \alpha_{max}} \tau_1(\alpha) = 4\cos(\alpha_{min}) f_{max}\\
\tau_{2max} &= \max_{\alpha_{min} \le \alpha \le \alpha_{max}} \tau_2(\alpha) = 4\sin(\alpha_{max}) f_{max}\\
\tau_{3max} &= \max_{\alpha_{min} \le \alpha \le \alpha_{max}} \tau_3(\alpha) = 4d f_{max}
\end{aligned} \tag{11}$$

for :

$$\alpha = \frac{\pi}{2} - \varphi$$

An analysis of Eq. (10) shows that the propulsive moment $\tau_3(\alpha)$ depends on the thrust angle α through the term $\sin(\alpha + \varphi)$, where the angle φ is a time - independent design parameter.

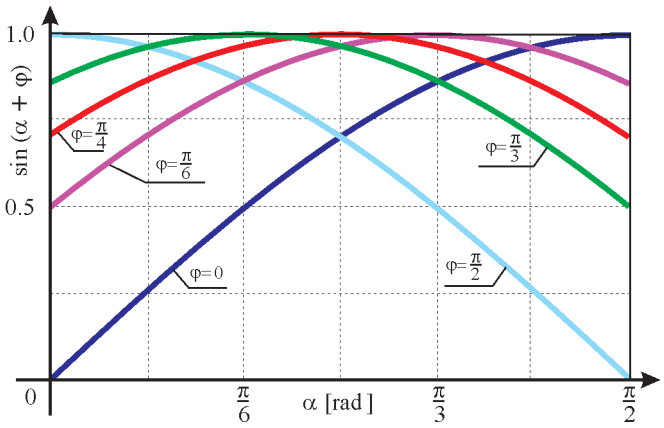

Fig. 5. *Influence of selected values of the angle φ on sin(a + φ) value*

In Fig.5 runs of the relationship $\sin(\alpha + \varphi)$ in function of the angle $\alpha \in (0, \frac{\pi}{2})$ are illustrated for some values of the angle φ contained in the interval $(0, \frac{\pi}{2})$. They demonstrate that for a fixed value of the angle φ it is possible to determine such value of the propulsive moment which can be always generated independently of a current value of the thrust angle α. The value is further marked τ_{3max} and calculated as follows :

$$\begin{aligned}
\tau_{3max} &< \min_{\alpha \in (\alpha_{min}, \alpha_{max})} \tau_3(\alpha) =\\
&= \begin{cases}
4d \sin(\alpha_{min} + \varphi) f_{max} & \text{for} \quad \varphi \in \left(0, \frac{\pi}{4}\right\rangle\\
4d \sin(\alpha_{max} + \varphi) f_{max} & \text{for} \quad \varphi \in \left(\frac{\pi}{4}, \frac{\pi}{2}\right)
\end{cases}
\end{aligned} \tag{12}$$

Therefore, by applying the following constraint onto the propulsive moment τ_{d3} :

$$\tau_{d3}^2 - \tau_{3max}^2 \leq 0 \tag{13}$$

its feasibility is ensured within the entire range of variability of the thrust angle α.

Values of the propulsive forces which should be developed by the propellers to generate the moment τ_{3max} independently of a value of the thrust angle α , are determined by the relationship:

$$f_{\tau_{3max}} = \begin{cases} \dfrac{\tau_{3max}}{4d\sin(\alpha_{min}+\varphi)} & \text{for} \quad \varphi \in \left(0, \dfrac{\pi}{4}\right\rangle \\ \dfrac{\tau_{3max}}{4d\sin(\alpha_{max}+\varphi)} & \text{for} \quad \varphi \in \left(\dfrac{\pi}{4}, \dfrac{\pi}{2}\right) \end{cases} \tag{14}$$

The reserving of a part of propeller's output to generate the force moment τ_{3max} makes that the maximum values of the forces τ_{1max} and τ_{2max} which can be generated by the propulsion system, will be smaller. Their new values marked τ_{1max} and τ_{2max}, respectively, are now :

$$\begin{aligned} \tau_{1max} &= 4\cos(\alpha_{min})\left(f_{max} - f_{\tau_{3max}}\right) \\ \tau_{2max} &= 4\sin(\alpha_{max})\left(f_{max} - f_{\tau_{3max}}\right) \end{aligned} \tag{15}$$

In further considerations it was assumed that :

$$\tau_d = [\tau_{d1}\ ,\ \tau_{d2}\ ,\ \tau_{d3}]^T$$

is the vector of set control inputs whose components satisfy the constraints :

$$\tau_{d1}^2 - \tau_{1max}^2 \leq 0\ ,\ \tau_{d2}^2 - \tau_{2max}^2 \leq 0\ ,\ \tau_{d3}^2 - \tau_{3max}^2 \leq 0$$

and P is a point of planar coordinates (τ_{d2}, τ_{d1}).

By analyzing the relationships (8) and (9) it was stated that the demanded propulsive forces τ_{d1} and τ_{d2} can be simultaneously generated by the propulsion system then and only then if the point P is located inside or at the edge of a geometrical figure shown in Fig.6. The figure is an asteroid described as follows :

$$\tau_1^{\frac{2}{3}} + \tau_2^{\frac{2}{3}} - \tau_{1max}^{\frac{2}{3}} = 0 \tag{16}$$

whose vertices are the points of the coordinates :

$(\tau_{2max}\ ,\ 0)$; $(0\ ,\ \tau_{1max})$; $(-\tau_{2max}\ ,\ 0)$

and $(0\ ,\ -\tau_{1max})$ respectively.

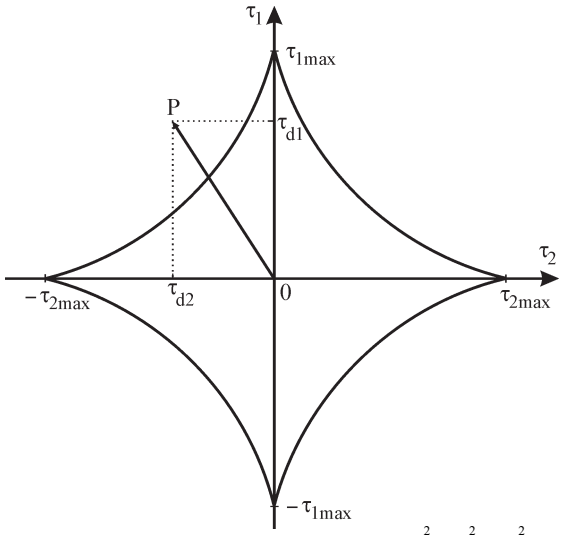

Fig. 6. *The asteroid described by the equation* $\tau_{d1}^{\frac{2}{3}} + \tau_{d2}^{\frac{2}{3}} = \tau_{1max}^{\frac{2}{3}}$, *and the position vector* OP

However if the point P lies outside the asteroid then the propulsion system is uncapable to develop set forces. Then the vector of permissible forces and moment $\boldsymbol{\tau}'_d = [\tau'_{d1}\ ,\tau'_{d2}\ ,\tau_{d3}\ ]^T$ and the corresponding thrust angle α' should be determined.

The schematic diagram of the algorithm for determining the permissible control inputs $\boldsymbol{\tau}'_d$ and the angle α' is shown in Fig.7. Input data for the algorithm are :

- the set vector of control inputs $\boldsymbol{\tau}_d$
- the maximum value of the propulsive force τ_{1max}
- a current value of the thrust angle α

and, the task of determining the permissible values of propulsive forces τ'_{d1} and τ'_{d2} as well as of the thrust angle α' is realized for the following conditions :

- the propulsive moment is kept unchanged : $\tau'_{d3} = \tau_{d3}$
- the mutual ratio of the forces : $\dfrac{\tau'_{d1}}{\tau'_{d2}} = \dfrac{\tau_{d1}}{\tau_{d2}}$ is maintained.

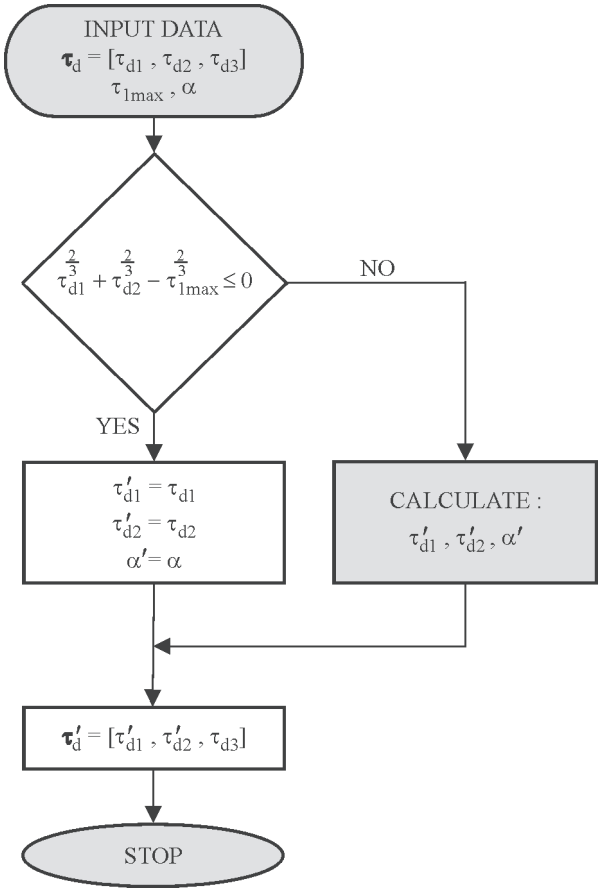

Fig. 7. *Schematic diagram of the algorithm for determining permissible control inputs and thrust angle*

The algorithm in question consists of the following steps :

1. ***Calculate the expression*** :

$$\tau_{d1}^{\frac{2}{3}} + \tau_{d2}^{\frac{2}{3}} - \tau_{1max}^{\frac{2}{3}} \leq 0 \tag{17}$$

to check whether the point $P = (\tau_{d2}\ ,\ \tau_{d1})$ lies inside or at the edge of the asteroid.

2. ***If the inequality*** **(17)** ***is true then apply substitutions*** :

$$\tau'_{d1} = \tau_{d1}$$

$$\tau'_{d2} = \tau_{d2}$$

$$\alpha' = \alpha$$

and go to Step 4.

3. ***If the inequality* (17) *is false then calculate*** :

$$\tau'_{d1} = \text{sign}(\tau_{d1})\left|\frac{\tau_{d1}}{\tau_{d2}}\right|\left(\left(\frac{\tau_{d1}}{\tau_{d2}}\right)^{\frac{2}{3}}+1\right)^{-\frac{3}{2}}\tau_{1max}$$

$$\tau'_{d2} = \text{sign}(\tau_{d2})\left(\left(\frac{\tau_{d1}}{\tau_{d2}}\right)^{\frac{2}{3}}+1\right)^{-\frac{3}{2}}\tau_{1max} \qquad (18)$$

$$\alpha' = \frac{\pi}{2} - \arctan\left(\left|\frac{\tau_{d1}}{\tau_{d2}}\right|^{\frac{1}{3}}\right)$$

4. ***Apply substitutions*** :

$$\boldsymbol{\tau}'_d = [\tau'_{d1}, \tau'_{d2}, \tau_{d3}]^T$$

5. ***The end of the algorithm***.

The proof of Eq. (18) can be found in [6].

Numerical example

Numerical calculations were carried out for the following data :

$\tau_d = [700\text{ N} \;;\; -120\text{ N} \;;\; 50\text{ Nm}]^T$

$\tau_{3min} = 50$ Nm , $f_{max} = 250$ N

$\varphi = 30°$, $d = 0.4$ m

The value of τ_{1max} was calculated for the worst case, i.e. for the angle $\alpha_{min} = 0°$:

$$\tau_{1max} = 4(f_{max} - f_{\tau_3}) =$$

$$= 4\left(250 - \frac{50}{4\cdot 0.4\cdot \sin(30°)}\right) = 750\,\text{N}$$

Step 1

Check if the point (τ_{d2} , τ_{d1}) lies inside or at the edge of the asteroid, i.e. check the condition (17) :

$$\tau_{d1}^{\frac{2}{3}} + \tau_{d2}^{\frac{2}{3}} - \tau_{1max}^{\frac{2}{3}} \le 0$$

$$700^{2/3} + (-120)^{2/3} - 750^{2/3} = 20.6 > 0$$

Step 2

As the inequality has appeared false the point (τ_{d2} , τ_{d1}) lies outside the asteroid. Calculate – by using (18) – permissible values of forces and thrust angle :

A. *Calculation of the value of the force* τ'_{d2}:

$$\tau'_{d2} = \text{sign}(\tau_{d2})\left(\left(\frac{\tau_{d1}}{\tau_{d2}}\right)^{\frac{2}{3}}+1\right)^{-\frac{3}{2}}\tau_{1max} =$$

$$= \text{sign}(-120)\left(\left(\frac{700}{-120}\right)^{\frac{2}{3}}+1\right)^{-\frac{3}{2}}750 = -85.9$$

B. *Calculation of the value of the force* τ'_{d1} :

$$\tau'_{d1} = \text{sign}(\tau_{d1})\left|\frac{\tau_{d1}}{\tau_{d2}}\right|\left(\left(\frac{\tau_{d1}}{\tau_{d2}}\right)^{\frac{2}{3}}+1\right)^{-\frac{3}{2}}\tau_{1max} =$$

$$= \text{sign}(700)\left|\frac{700}{-120}\right|\left(\left(\frac{700}{-120}\right)^{\frac{2}{3}}+1\right)^{-\frac{3}{2}}750 = 501$$

C. *Calculation of the value of the angle* α' :

$$\alpha' = \frac{\pi}{2} - \arctan\left(\left|\frac{\tau_{d1}}{\tau_{d2}}\right|^{\frac{1}{3}}\right) =$$

$$= \frac{\pi}{2} - \arctan\left(\left|\frac{700}{-120}\right|^{\frac{1}{3}}\right) = 0.51\,\text{rad} = 29.1°$$

Step 3

Calculation of the vector of permissible control inputs :

$$\boldsymbol{\tau}'_d = [501 \;;\; -85.9 \;;\; 50]$$

To assess correctness of the calculations it was checked if the ratio of longitudinal and transverse forces was kept unchanged:

$$\frac{\tau_{d1}}{\tau_{d2}} = \frac{700}{-120} = -5.83 \quad ; \quad \frac{\tau'_{d1}}{\tau'_{d2}} = \frac{501}{-85.9} = -5.83$$

The obtained result showed that after correction the ratio of the forces was of the same value.

RECAPITULATION

- The presented paper concerns synthesis of an automatic control system for unmanned underwater robot, particularly its phase connected with power distribution in multi-propeller propulsion system. Planar horizontal motion of the robot executed by means of four azimuth propellers was considered.
- For thrust allocation to the propellers an unconstrained optimization method was applied. To use the method practically in a propulsion system of a limited power output a procedure which makes it possible to assess its capability of generating demanded forces and moment was elaborated.
- For the case when the task appears unfeasible an algorithm was proposed allowing to modify propulsive forces by proportional decreasing their values and determining permissible ones, i.e. the forces which the propulsion system is capable to develop.
- The performed numerical tests confirmed correctness of the applied approach.

NOMENCLATURE

d_i – distance from i-th propeller to robot's mass centre
f_i – i-th propeller's thrust
f – vector of thrusts
K – propulsive moment around longitudinal axis of hull-fixed reference system

M – propulsive moment around transverse axis of hull-fixed reference system
N – propulsive moment around vertical axis of hull-fixed reference system
p – angular velocity around longitudinal axis of hull-fixed reference system
q – angular velocity around transverse axis of hull-fixed reference system
r – angular velocity around vertical axis of hull-fixed reference system
t – time
$\mathbf{T}(\mathbf{a})$ – arrangement matrix of propellers
u – linear velocity along longitudinal axis of hull-fixed reference system
$\mathbf{v}$ – vector of linear and angular velocities in hull-fixed reference system
w – linear velocity along vertical axis of hull-fixed reference system
x – x – coordinate of vehicle's position in inertial reference system
X – propulsive force along longitudinal axis in hull-fixed reference system
y – y – coordinate of vehicle's position in inertial reference system
Y – propulsive force along transverse axis in hull-fixed reference system
z – z – coordinate of vehicle's position in inertial reference system
Z – propulsive force along vertical axis in hull-fixed reference system

α_i – i-th propeller thrust angle
$\boldsymbol{\eta}$ – vector of location and orientation of vehicle in inertial reference system
θ – heel angle
ν – linear velocity along transverse axis of hull-fixed reference system
$\boldsymbol{\tau}$ – vector of propulsive moments and forces
$\boldsymbol{\tau}_d$ – vector of demanded propulsive moments and forces
φ_i – i-th propeller orientation angle
ϕ – trim angle
ψ – course angle

BIBLIOGRAPHY

1. Fossen T.I.: *Guidance and Control of Ocean Vehicles*. John Wiley and Sons. Chichester, 1994
2. Fossen T.I.: *Marine Control Systems.* Marine Cybernetics AS. Trondheim, 2002
3. Garus J.: *Kinematical Control of Motion of Underwater Vehicle in Horizontal Plane.* Polish Maritime Research, Vol. 11, No. 2/2004
4. Garus J.: *A Method of Determination of Control Inputs Limit for Remotely Operated Vehicle.* Proc. of the 10th IEEE (the Institute of Electrical and Electronics Engineers, Inc.) Int. Conf. on Methods and Models in Automation and Robotics MMAR'2004, Międzyzdroje (Poland), 2004
5. Garus J.: *Optimization of Thrust Allocation in the Propulsion System of an Underwater Vehicle*. Int. Journal of Applied Mathematics and Computer Science, Vol. 14, No. 4/2004
6. Garus J.: *Power distribution control in propulsion system of underwater vehicle* (in Polish). Zeszyty Naukowe AMW (Scientific Bulletins of Polish Naval University), No. 160B/2005

CONTACT WITH THE AUTHOR

Jerzy Garus, D.Sc.,Eng.
Department of Mechanical and Electrical Engineering,
Polish Naval University
Śmidowicza 69
81-103 Gdynia, POLAND
e-mail : j.garus@amw.gdynia.pl

Conference

MECHANIKA 2005

On 4 February 2005,
Mechanical Faculty,
Gdańsk University of Technology,
organized the Scientific Conference :

Mechanika

on the occasion of 60th anniversary of its activity.

Such conferences were earlier arranged in the years 1995, 1997 and 1999. Their idea was to promote achievements of scientific workers from mechanical faculties of the technical universities located in North Poland, i.e. in Gdańsk, Gdynia, Szczecin, Koszalin, Bydgoszcz, Olsztyn, Białystok and Elbląg., as well as of the Institute of Fluid Flow Machinery, Polish Academy of Sciences, Gdańsk. It was mainly expected to draw interest of industrial enterprises of that region to those achievements. However effects of the attempts appeared unsatisfactory as technological parks, industrial fairs and branch conferences have become more effective occasions for contacts between scientific and industrial circles.

As a result of the situation, this-year Conference was devoted to mutual presentation of selected research results and discussion on prospects of development of mechanical sciences within the frame of developing international cooperation.

In compliance with the Conference's program 35 papers were presented during three topical sessions :

- ***Techniques and engineering processes of manufacturing*** (12 papers)
- ***Drives and energy systems*** (12 papers)
- ***Computer methods in mechanics*** (11 papers).

Representatives of the Conference's organizer - - with 17 papers - contributed the most to the elaboration of the presented papers.

The remaining ones were prepared by authors from :

the Faculty of Ocean Engineering and Ship Technology – – Gdańsk University of Technology, Olsztyn Technical Agricultural Academy, Białystok University of Technology, Technical University of Szczecin, Warmia-Mazury University, Institute of Fluid-Flow Machinery of PAS – – Gdańsk, Koszalin University of Technology, Polish Naval University, the State Higher School of Engineering in Elbląg, and ALSTOM company.

60th Anniversary

Jubilee Academic Year 2004/2005

The years 1945÷2005 have been a period of dynamical development of Gdańsk University of Technology which has today become the greatest technical university in the northern region of Poland. The University may be proud of graduating over 80 thousand engineers in many disciplines, and of many achievements in the area of scientific research. The University's employees have taken part in the activity of many international scientific associations and they have organized many times international conferences giving impact to development in many domains of contemporary science.

Gdańsk University of Technology - main building (photo: C. Spigarski)

These achievements justify undertaking a very comprehensive, almost a forthnight lasting programme of celebration of 60th anniversary of that so much mertorious university. Beginning from the end of May this year many historical and scientific conferences, cultural events and light programmes were held. It was also an exceptional occasion for arranging a gaudy-day of the university's graduates to give them an opportunity to meeting in close circles of colleagues.

Among nine today existing faculties of the University six of them have celebrated their own jubilee of 60th anniversary because in 1945 they formed an origin for the further development of the University.

The Faculty of Ocean Engineering and Ship Technology (formerly Faculty of Shipbuilding) also belonged to that group. The Faculty much contributed to dynamical development of shipbuilding industry in Poland, which built more than 5000 ships of different types, among which a dozen or so was distinguished by international maritime bodies.

Within the frame of the celebration programme of the Faculty's jubilee, was held a solemn open session of the Faculty Council devoted to history of activity of the Faculty.

- Education of many engineers and scientific workers with scientific degrees was acknowledged as the greatest achievement of the Faculty. As many as 2226 B.Sc.diplomas and 3409 M.Sc. diplomas together were issued in the specialties of : Building of Sea-going Ships, Building of Inland Waterways Ships, Ship Power Plants and Machines, Ship Equipment, Ship Technical Operation, Management and Marketing in Maritime Economy. Also, 329 doctoral studies were completed.
- The 60 - year history of the Faculty has been described in the carefully edited book of 410 pages, titled : „*Shipbuilding studies at Gdańsk University of Technology in the years 1945÷2005*".
- The Faculty's graduates have been a basic, highly appreciated group of specialists employed in Polish industrial enterprises and shipping companies; many of them have carried out a fruitful didactic and scientific activity at the universities.
- A number of them have worked for foreign firms outside Poland. Some of them, namely Mr. T. Berżowski, E. Haciski, T. Jaroszyński, W. Kossakowski, L. K. Kupras, R. Scheinberg and Z. K. Wójcik have imparted a piece of remembrance just on their proffessional activity in various parts of the world.
- Finally, a solemn accent of the celebration was the ceremony of giving the Faculty's modern laboratory for fuel oils and lubricants the name of **Prof**. **Janusz Staliński**, deceased in 1985 former Rector of the University, Dean of the Faculty and multi-year Head of the Department of Ship Power Plants. Prof. Staliński gave a great impact to the Department's development in respect to its didactic, scientific and design activities. He tightly cooperated both with industrial enterprises and shipping companies, that favourably influenced the course of studies in the field of ship power plants.

Faculty of Ocean Engineering and Ship Technology